2020

Small RNAs: Big Roles in White Mold Infecting Crop Plants

Achal Neupane
South Dakota State University

SMALL RNAS: BIG ROLES IN WHITE MOLD INFECTING CROP PLANTS

BY

ACHAL NEUPANE

A dissertation submitted in partial fulfillment of the requirements for the

Doctor of Philosophy

Major in Biological Sciences

Specialization in Microbiology

South Dakota State University

2020

DISSERTATION ACCEPTANCE PAGE

Achal Neupane

This dissertation is approved as a creditable and independent investigation by a candidate for the Doctor of Philosophy degree and is acceptable for meeting the dissertation requirements for this degree. Acceptance of this does not imply that the conclusions reached by the candidate are necessarily the conclusions of the major department.

Dr. Shin-Yi Lee Marzano
Advisor Date

Volker Brozel
Department Head Date

Dean, Graduate School Date

This dissertation is dedicated to my mother Madhavi Sharma and my late father Rabindra Nath Sharma. I also dedicate this work to my sister Akangkshya Sharma and my beloved wife Yamuna Dhungana.

ACKNOWLEDGEMENTS

I would like to thank my advisor Dr. Shin-Yi Lee Marzano for all the support and guidance she has provided throughout my PhD research. I am also thankful to her for giving me opportunity to work on multiple projects to be trained as a bioinformatics researcher. I am grateful to Drs. Senthil Subramanian, Madhav Nepal, Stephanie Bruggeman, Yajun Wu and Larry Browning for providing constructive feedback and support throughout my PhD program.

I am thankful to the Department of Biology and Microbiology at South Dakota State University and Drs. Clay for providing me with the necessary support for the completion of my PhD program. I am also thankful to the staff at High Performance Computing at SDSU for their help in my research.

CONTENTS

ABSTRACT

SMALL RNAS: BIG ROLES IN WHITE MOLD INFECTING CROP PLANTS

ACHAL NEUPANE

2020

In eukaryotes, small RNAs (sRNAs) are key regulators of RNA silencing which is also known as RNA interference (RNAi). RNAi is an essential mechanism known in plants, animals and fungi that regulates various biological activities, including defense against foreign nucleic acids and viruses. Fungal pathogens, such as *Sclerotinia sclerotiorum*, severely limit crop production in all parts of the world. *Sclerotinia sclerotiorum* cause white mold infection, affecting all dicotyledonous plants including many economically important field crops, vegetables, and floriculture. There does not exist known host resistance, and only limited chemical control can be achieved. Given the growing cost and environmental impacts of using fungicides to control these pathogens, an alternative method that exploits RNA silencing in fungi is warranted.

The objectives of my research were: (i) to understand RNA-editing mechanism in virus derived small interferring RNAs (VsiRNAs), (ii) to discover mycoviruses from metatranscriptomic study of arbuscular mycorrhizal fungus *Rhizophagus* spp., and (iii) to characterize the antiviral roles of RNAi genes in *S. sclerotiorum*. This dissertation includes three chapters from my PhD research. In chapter 1, I have demonstrated that RNA editing mechanism is common in fungi, including *S. sclerotiorum*, *Botrytis cinerea*, and *Fusarium graminearum*, as well as in higher metazoans. My analysis showed that the virus-infected wild-type and RNAi mutant strains of *S. sclerotiorum* accumulate virus-derived small RNAs with distinct patterns of internal and terminal modifications. Chapter

2 deals with the discovery of mycoviruses infecting arbuscular mycorrhizal fungus and their evolution with respect to their counterparts infecting pathogenic fungi. Finally, chapter 3 focuses on the characterization of RNAi genes in *S. sclerotiorum*.

While RNA silencing in fungi is primarily involved in antiviral defense against foreign nucleic acids, pathogenic fungi also utilize RNA silencing mechanism to silence host defense genes in plants through the delivery of small RNA molecules as virulence effectors. Beginning with the discovery of RNA editing events, this study investigates the roles of RNAi genes in fungal pathogen *S. sclerotiorum* using various approaches in bioinformatics.

The present study dissects the RNA silencing pathway in *S. sclerotiorum* by disrupting its key silencing genes using the split-marker recombination method in order to probe the contributions of these genes, specifically argonautes, to fungal virulence and viral defense mechanisms. Following gene disruption, mutants were studied for changes in phenotype, pathogenicity, viral susceptibility, and small RNA processing compared to the wild-type strain, DK3. Among the *argonaute* mutants, the Δ*agl*-2 mutant had significantly slower growth and virulence prior to and following virus infection. Additional analyses indicated that the virus-infected wild-type strain accumulated virus-derived small RNAS (vsiRNAs) with distinct patterns of internal and terminal nucleotide mismatches. Δ*dcl*-1 mutant produced less vsiRNA compared to Δ*dcl*-2 mutant and the wild type strain, suggesting the two dicers are not in the state of complete redundancy.

An emerging area of interest is the use of external dsRNA-based pest control which will require detailed characterization of the RNA silencing pathways in *S. sclerotiorum*. In an attempt to investigate the utility of dsRNA-based pest control strategy

for white mold, we studied the roles of argonaute enzymes, *agl*-2 and *agl*-4, in small RNA metabolism in *S. sclerotiorum*. Our study has shown that RNA silencing deficient *S. sclerotiorum* show increased susceptibility to virus infection. Additionally, we also profiled different classes of small RNAs, including vsiRNAs, from different gene mutants to study viral susceptibility, internal modification, stability, and small RNA processing compared to wild-type strain, DK3, of *S. sclerotiorum*.

Results from this study show that fungal pathogen *S. sclerotiorum* host robust RNA silencing mechanisms to defend against foreign nucleic acid and viruses and to facilitate fungal infection of host plants through trans-kingdom RNAi. These findings expand our overall understanding of *S. sclerotiorum* and has important implications for any current or future uses of dsRNA and mycoviruses as disease control agents.

CHAPTER ONE: RNA-EDITING OF VIRUS-DERIVED SMALL INTERFERING RNAS (VSIRNAS)

Abstract

RNA silencing, also known as RNA interference, is an essential mechanism in plants, animals and fungi that functions in gene regulation and defense against foreign nucleic acids. In fungi, RNA silencing has been shown to function primarily in defense against invasive nucleic acids. RNA-silencing- deficient fungi show increased susceptibility to virus infection. Although RNA-editing in plants and animals have been well studied, RNA-editing in fungi is a fairly new concept. Also, very little is known about the classes of RNA editing in virus-derived small interfering RNA (vsiRNA) which will teach us the nature of self-nonself recognition and ways to modulate RNA modification to control fungal infections. This study will help us understand evolutionarily conserved antiviral defense mechanism in *S. sclerotiorum*, and fungal pathogens in general.

1.1 RNA silencing in *Sclerotinia sclerotiorum*

RNA interference (RNAi) or RNA silencing is a mechanism essential to eukaryotes in regulating gene functions through transcriptional and posttranscriptional suppression of gene expression. RNAi was first discovered in 1998 (Fire et al., 1998) and since then it has been shown to play important roles in regulating gene expression involving mRNA degradation, inactivation of translation and chromatin remodeling (Nakayashiki et al., 2006). RNA silencing requires dsRNA or hairpin RNAs processed into short 21-24nt long RNA molecules processed by RNase-III endonucleases (also known as dicers) (Baulcombe, 2002;Baulcombe, 2004). Depending on the source, these

small RNA molecules which can be either small interfering RNA (siRNA) or microRNA (miRNA), form a complex with Argonaute proteins known as RNA-induced silencing complexes (RISCs) that direct degradation or translational repression of complementary RNA sequences (Baulcombe, 2002;Baulcombe, 2004;Baulcombe, 2005;Bouche et al., 2006;Dang et al., 2011).

RNAi in fungi is an adaptive defense strategy by which invasive nucleic acids are inactivated or degraded. While RNA silencing in animals and plants is essential for survival of the organism, it has been shown that, in fungi, RNA silencing is vital only as part of the defense strategy, such as against virus infection (Segers et al., 2007). Nonetheless, studies have shown that filamentous fungi have diverse small RNA biogenesis pathways that are activated in response to different cellular processes for which some of the RNA silencing genes have more than one functions (Dang et al., 2011) while other could have redundant roles, particularly in antiviral processing of dsRNA or transgenes (Catalanotto et al., 2004;Wang et al., 2016a). *Sclerotinia sclerotiorum* (white mold fungus) is one of the major plant pathogens that could cause up to 100% loss in crop yield and is also known to affect a wide range of crop species (Heffer Link and Johnson, 2007). Studies have shown that RNA silencing is an important measure fungal pathogens take to defend against foreign nucleic acids (such as mycoviruses), and also to establish pathogenesis against host organisms (Amselem et al., 2011;Wang et al., 2016a;Mochama et al., 2018). RNA silencing pathway involves various genes, such as argonaute, dicer and RNA-dependent-RNA-polymerase (RDRP) and their number in fungi differs even within the two species of same genera. For example, within the same genus, *Ustilago maydis* have RNA silencing genes while *Ustilago hordei* does not have

any RNA silencing genes (Laurie et al., 2012). RNA silencing in *S. sclerotiorum* is comprised of two *argonautes* genes (*ago*-2 and *ago*-4), two *dicer* genes (*dcl*-1 and *dcl*-2) and three RDRP genes (Laurie et al. (2012).). Our recent studies of gene disruption mutants of argonaute (Δ*agl*-2 and Δ*agl*-4) and dicer (Δ*dcl*-1, Δ*dcl*-2 and ΔΔ*dcl*-1/2) showed different phenotypic, virulence, viral susceptibility and small RNA accumulation responses with and without virus infection (Mochama et al., 2018;Neupane et al., 2019). In double dicer mutants (ΔΔ*dcl*-1/2), *S. sclerotiorum* showed reduced pigmentation, reduced sclerotial formation, reduced small RNA (sRNA) production, severe debilitation following virus infection and eliminated vsiRNA production while these changes were not seen in single dicer mutants (Mochama et al., 2018). Similarly, the *argonaute*-2 mutant (Δ*agl*-2) exhibited slower growth prior to virus infection, significantly smaller lesion size and greater debilitation under virus infection while *argonaute*-4 (Δ*agl*-4) mutants did not exhibit phenotypic changes (Neupane et al., 2019). This also confirms that some RNA silencing genes in *S. sclerotiorum* have diverse and essential roles while other genes remain functionally redundant.

1.2 Biogenesis of virus-derived small interfering RNAs (vsiRNAs)

In eukaryotes, including in fungi, small RNAs are known as key players of RNA silencing that regulate various biological processes. Many of these silencing components involve processing of double-stranded RNAs (dsRNAs) that are often generated by host or virus related RNA-dependent RNA polymerases into 21-26 nucleotide sequences known as small interfering RNAs (siRNAs) (Hamilton and Baulcombe, 1999;Elbashir et al., 2001). Long precursor dsRNAs are then cleaved by a member of RNase III family of nucleases called dicer which specifically targets double-stranded RNAs (Bernstein et al.,

2001). These dsRNA-processed small RNAs are repressor of gene expression that are common to RNA silencing in plants, higher metazoans and fungi (Baulcombe, 2002). These siRNAs are incorporated into argonaute proteins to form RNA-induced silencing complex (RISC) that guides through the target single-stranded RNAs of the corresponding dsRNA for post-transcriptional silencing (Zamore, 2001;Hock and Meister, 2008). In plants, shorter siRNAs (21-22 nucleotide long sequences) are more abundant and are primarily involved in the degradation of mRNAs while longer (24-26 bases long) counterparts are involved in regulating DNA methylation and systemic silencing (Hamilton et al., 2002). The major contrast with miRNA to this class of small RNA is that miRNAs are generated from miRNA genes that generate a single-stranded RNA transcript with a stem-loop structure which is then recognized and processed by dicers (Bouche et al., 2006;Dang et al., 2011). Additionally, miRNAs can degrade mRNA targets that are nearly perfect complementary while siRNAs target fully complementary transcripts and are primarily part of defense mechanism (Dang et al., 2011).

In plants, four subgroups of siRNAs have been reported, namely, *trans*-acting siRNAs (ta-siRNAs), heterochromatic-associated siRNAs (hc-siRNAs), natural antisense transcript siRNAs (nat-siRNAs), and virus-activated siRNAs (vasiRNAs) (Zhang et al., 2015). Additionally, virus derived-small interfering RNAs (vsiRNAs) have also been found in various organisms that are generated in response to antiviral immunity against viral genomic RNA (Zhu and Guo, 2012). In plants, each dicer is responsible for generating vsiRNAs of specific sequence lengths, and only DCL2 and DCL4 are actively involved in processing majority of vsiRNAs after virus infection (Deleris et al., 2006;Zhu and Guo, 2012). Additionally, two different classes of vsiRNAs have been reported: the

primary vsiRNAs that are cleaved by dicer immediately after viral RNA triggers are detected, and secondary vsiRNAs generated from resulting viral fragments that are often processed into dsRNA by RNA-dependent RNA polymerase (RDRP) enzymes and then recognized and processed by dicers (Dunoyer et al., 2005;Wassenegger and Krczal, 2006).

In fungi, RNA silencing is particularly important in defense against viruses. As seen in *Cryphonectria parasitica* (a close relative of *Neurospora crassa*), infection with Cryphonectria hypovirus 1 (CHV1) reduces the virulence of the fungal host (Nuss, 2005) by utilizing papain-like protease (p29) which is a viral suppressor of RNA silencing in fungal and plant hosts (Suzuki et al., 2003). Generation of siRNAs is an important feature of RNA silencing reported in plants, animals (Zamore, 2002), and fungal species, such as *N. crassa* (Catalanotto et al., 2002), *Magnaporthe oryzae* (Kadotani et al., 2003), and *Aspergillus nidulans* (Hammond and Keller, 2005). Filamentous fungi host the replication of numerous mycoviruses with both dsRNA or plus-sense ssRNA genomes and some of which also have sequence similarities with viruses infecting plants (Pearson et al., 2009). In this regard, virus-derived small interfering RNAs (vsiRNAs) are associated with RNAi pathways directing antiviral immunity in fungi (Ding and Voinnet, 2007;Aliyari and Ding, 2009). Biogenesis of vsiRNA in fungi is similar to that of endogenous small RNA that involves different RNAi proteins including dicers, argonautes, and RDRPs. The biogenesis of vsiRNA is becoming clearer through Next generation sequencing of small RNAs and bioinformatics analysis of different RNAi mutants. In this study, I will discuss some of our research findings on RNA-editing in

vsiRNAs based on the analysis of small RNA-seq, RNA-seq and degradome-seq data analysis.

1.3 RNA-editing

The concept of RNA-editing was first explored in mid-1980s to describe the mechanisms by which uridine is inserted into the mitochondrial cytochrome oxidase (cox) subunit II of trypanosomatid (Benne et al., 1986). Since then, RNA-editing has been a widely studied mechanism that governs several RNA processing events related to gene function, growth, defense and survival of organisms.

One of the most common editing events include adenosine-to-inosine (A-to-I) modification mediated by adenosine deaminase protein family members (ADAR) acting on RNA. Inosine is known to be interpreted as guanosine by cellular machinery (Basilio et al., 1962). ADAR mediated RNA-editing acts on double-stranded RNA (dsRNA) even without perfect complementarity (Nishikura, 2010), and causes deamination of almost half of all adenosine residues with perfect complementarity (Polson and Bass, 1994). ADAR editing could be highly site selective when mediated by ADAR2 compared to more random editing by ADAR1 (Kallman et al., 2003). Site selective editing is determined also by the immediate structure and residues surrounding the editing sites. For example, for a purine (A or G) opposite to the editing site has negative affinity on both selectivity and efficiency because purines bases are comparatively larger than pyrimidines and could sterically interfere with the target (Wong et al., 2001;Kallman et al., 2003). ADAR mediated editing is common among cellular pre-mRNA, viral RNA and non-coding RNA-editing (Gerber and Keller, 2001). While ADAR mediated RNA-editing is common in metazoans (and particularly in mammals) (Savva et al., 2012), it

has not been found in a variety of non-metazoan eukaryotes like plant and fungal species (Jin et al., 2009). Although, yeasts and filamentous fungi lack the orthologs of ADAR, they still have A-to-I editing independent of ADAR enzymes. For example, A-to-I editing found in *Fusarium graminearum* seems to be independent of ADAR and have sequence preference and site selectivity for editing which is different from animals (Liu et al., 2016).

Similarly, prokaryotes do not have ADAR genes, but their evolutionarily more ancestral counterparts, transfer RNA (tRNA) adenosine deaminase (TadA) are responsible for tRNA specific modifications (Wolf et al., 2002). Orthologs of TadA in eukaryotes is known as adenosine deaminases acting on tRNAs (ADATs) and mediate deamination of A-to-I editing targeting tRNA anticodon (Gerber and Keller, 2001). Sequence homology analysis between the catalytic domains associated with ADARs and ADATs also indicates that the ADATs are ancestral to ADARs (Savva et al., 2012). This suggests that the ADAR-mediated RNA-editing mechanisms in higher metazoans and mammals are recently evolved from ADATs. In *F. graminearum*, out of three ADAT genes (*FgTAD1*, *FgTAD2* and *FgTAD3*), only *FgTAD2* and *FgTAD3* contain cytidine/deoxycytidylate deaminase domain which suggests that only two of these genes are involved in A-to-I editing (Liu et al., 2016). Other filamentous fungi, such as *Neurospora crassa*, also seem to have novel RNA-editing that are independent of ADARs with stage-specific editing events at various sexual developmental stages (Liu et al., 2017), including editing of gene involved in fungal fruiting body development (Wang et al., 2014). Unlike in mammals, majority of these editing sites in *N. crassa* were found in coding regions altering amino acids, and since non-synonymous editing in *N. crassa*

are generally conserved, nearly 50% of these non-synonymous editing sites were also common to editing sites found in *N. tetrasperma* (Liu et al., 2017). Stage-specific A-to-I RNA-editing that regulates sexual reproduction is also common in *F. verticillioides* and perhaps many other *Sordariomycetes* (Sikhakolli et al., 2012;Liu et al., 2016).

Another class of RNA-editing is mediated by "Apolipoprotein B mRNA-editing enzyme, catalytic polypeptide-like" family of enzymes (also known as activation-induced deaminase AID/APOBEC family) which mediates deamination of cytosine to uracil (C-to-U) commonly affecting protein coding, ribosomal and tRNAs in different organisms (Mahendran et al., 1991;Navaratnam et al., 1998;Lerner et al., 2018). Among several members of APOBEC family, APOBEC1 was the first discovered enzyme which deaminates a certain cytosine residue in the sequence of apolipoprotein B (Apob) pre-mRNA (Teng et al., 1993). This enzyme has been shown to mediate the C-to-U editing that modifies a CAA codon to a stop codon which produces a shorter form of the APOB protein known as APOB-48 (Navaratnam et al., 1993;Teng et al., 1993). All members of AID/APOBEC family are evolutionarily conserved, share same structural residues comprised on zinc-dependent deaminase, and involved in (except for APOBEC2 and APOBEC4) C-to-U deaminase activity on single-stranded DNA or RNA (Lerner et al., 2018). APOBEC mediated deamination has been found in fungal species, *Ganoderma lucidum* (Zhu et al., 2014). Although most of the RNA-editing mechanisms in fungi is not as clear as in higher metazoans, their roles in fungal species could further elucidate the possible implications in fungal pathogen control strategy.

In human, viral dsRNA replicative intermediates trigger the production of vsiRNA that are loaded into argonaute protein to degrade cognate viral RNA sequences

(Qiu et al., 2017). In severe acute respiratory syndrome coronavirus (SARS-CoV) study done in human, synthetic siRNAs are found to downregulate the expression of SARS-CoV in a dose-dependent manner by targeting sequence-specific genes (Shi et al., 2005). Additionally, the thermodynamic stabilities of each strand of siRNA duplex (particularly for bases at the 5' end) determine the structural symmetry of siRNAs eligible for assembly into RISC and therefore also determine the overall function of siRNA molecules (Khvorova et al., 2003;Schwarz et al., 2003). Functionally active siRNA duplexes have lower internal stability at the 5'-antisense terminal base pair end compared to nonfunctional duplexes (Shi et al., 2005). When inactive siRNA duplexes are mutated at 21 base position of the positive strand to unpair with the 5' end of negative strand, they can downregulate the expression of cognate genes more efficiently (Shi et al., 2005).

1.4 Materials and Methods

1.4.1 Analysis of the Sequencing Data

Sequenced small RNA-seq data for virus-infected *S. sclerotiorum* Δ*ago*-2, Δ*dcl*-1 and Δ*dcl*-2 mutants were obtained from our previous studies (Mochama et al., 2018;Neupane et al., 2019), including virus-infected wild-type controls from (Lee Marzano et al., 2018;Neupane et al., 2019). RNA-Seq libraries of five virus-infected *S. sclerotiorum* were obtained from our previous study (Lee Marzano et al., 2018); NCBI accession: SRR8305679. To investigate the prevalence of RNA-editing in other organisms infected with their viruses, we also analyzed small RNA-seq datasets from SRA database (https://www.ncbi.nlm.nih.gov/sra/) for *Botrytis* (Donaire and Ayllon, 2017) under accessions: SRR3659825, SRR3659826, SRR3659827); *Fusarium* (Wang et al., 2016b) under accession: SRR3055827; mouse (Li et al., 2013) under accessions: SRR2175652, SRR2175613, SRR2175618); and human (Qiu et al., 2017) under

accessions: SRR5593145, SRR5593146, SRR5593147 and SRR5593148). Adaptors from small RNA-seq data were trimmed using BBDuk tool available from BBTools (Bushnell, 2014). ShortStack (Axtell, 2013) was used to identify loci producing sRNAs by clustering. The number of reads aligned to Sclerotinia sclerotiorum hypovirus 2 L (SsHV2-L) genomes were computed using Bowtie (Langmead et al., 2009). RNA-editing in small RNA reads were determined by allowing one mismatch for Bowtie (Langmead et al., 2009) alignment of 18-24 bases reads with SsHV2-L genome and further downstream analyses were performed using in-house Perl and R scripts. RNA-seq data were assembled using Trinity (Grabherr et al., 2011) to further validate the editing sites found in vsiRNAs from small RNA libraries of *S. sclerotiorum*.

1.5 Results and Discussion

1.5.1 Virus-derived small RNAs in *Sclerotinia sclerotiorum*

A wide range of editing was found in virus-derived small RNA species of various lengths obtained from small RNA libraries of *S. sclerotiorum* infected with SsHV2-L. Different amounts of vsiRNAs were produced by gene disruption mutants and wild-type *S. sclerotiorum* infected with SsHV2-L: Δ*ago*-2 at 5.64% and 6.59%, Δ*dcl*-1 at 2.77% and 3.97%, Δ*dcl*-2 at 16.61% and 13.86% and wild-type at 7.43% and 5.15% of the total reads in each library (Table 1). Based on the percentages, vsiRNA production seems to be mediated more by DCL1 compared to DCL2. While strand-bias was not observed in wild-type samples, vsiRNAs in gene-disruption mutants had alignment bias towards either positive or negative strands. Single-base RNA modification was relatively higher in gene-disruption mutants (13 - 22% of vsiRNAs) compared to only ~5% of the

vsiRNAs in wild-type (Table1). Additionally, RNA modification in 22nt sequences was most abundant (followed by 23nt and 21nt sequences) for all libraries.

Table 1. Number of mismatches in virus-derived small interfering RNAs (vsiRNAs) produced by virus-infected gene-knockout mutants (Δ*ago*-2, Δ*dcl*-1 and Δ*dcl*-2) and wild-type (Vmicro) *Sclerotinia sclerotiorum*. Percentage (%) in brackets is the percent of total reads in each library. Number of mismatches (both internal and terminal) are shown under column "Mismatches". Small RNA reads were aligned to Sclerotinia sclerotiorum hypovirus 2 L (SsHV2-L) genome.

Samples	Read Length	Mismatches	Total Mismatches (% of aligned reads)	Aligned Reads		Aligned Reads	Unaligned Reads
				Positive	Negative		
Δ*ago*-2_SsHV2L (Replicate1)	18	1229	148101 (22.31%)	255301 (38.46%)	408478 (61.54%)	663779 (5.64%)	11108069 (94.36%)
	19	4112					
	20	12420					
	21	27232					
	22	61841					
	23	33280					
	24	7987					
Δ*dcl*-1_SsHV2L (Replicate1)	18	1536	51603 (13.03%)	238027 (60.07%)	158202 (39.92%)	396229 (2.77%)	13918611 (97.23%)
	19	2502					
	20	4846					
	21	7578					
	22	11055					
	23	14015					
	24	10071					
Δ*dcl*-2_SsHV2L (Replicate1)	18	6756	779914 (19.05%)	1086244 (26.54%)	3005687 (73.45%)	4091931 (16.61%)	20541117 (83.39%)
	19	19596					
	20	53889					
	21	132785					
	22	347047					
	23	186372					
	24	33469					
Δ*ago*-2_SsHV2L (Replicate2)	18	1272	160427 (20.6%)	280845 (36.06%)	497871 (63.93%)	778716 (6.59%)	11042345 (93.41%)
	19	4251					
	20	13901					
	21	30055					
	22	69720					
	23	34929					
	24	6299					
Δ*dcl*-1_SsHV2L (Replicate2)	18	949	86603 (17.97%)	153947 (31.95%)	327873 (68.04%)	481820 (3.97%)	11661457 (96.03%)
	19	2565					
	20	7375					
	21	16656					
	22	39924					
	23	16388					
	24	2746					
	18	3720	488546 (18.92%)	634071 (24.56%)	1946815 (75.43%)	2580886 (13.86%)	16034792 (86.14%)
	19	11203					

Δ*dcl*-2 _SsHV2L (Replicate2)	20	30577					
	21	76081					
	22	222558					
	23	122516					
	24	21891					
1Vmicro (Replicate1)	18	1276	145191 (5.38%)	1335881 (49.52%)	1361468 (50.47%)	2697349 (7.43%)	33582701 (92.57%)
	19	3044					
	20	9889					
	21	26432					
	22	66488					
	23	30452					
	24	7610					
2Vmicro (Replicate2)	18	828	81277 (5.13%)	790405 (49.89%)	793766 (50.10%)	1584171 (5.15%)	29192922 (94.85%)
	19	1931					
	20	5475					
	21	14660					
	22	34691					
	23	18575					
	24	5117					

Both internal and terminal modifications were found in vsiRNAs produced by *S. sclerotinia* (Table 2 and Figure 1).

These modifications were primarily A-to-G at the 7th base of 18 bases long sequences, G-to-A at the 9th base of 23 bases long sequence, G-to-A at the 11th base of 22 bases long sequences along with the abundance of terminal modifications (Figure 1). These modifications were found in both replicates of our small RNA-seq data (Figure 1). Since these modifications are in relatively higher rates (Table 1), we think that these presumed edit sites in vsiRNAs are not the result of inherent sequencing error (NGS has error rates of <1% (Salk et al., 2018)). Additionally, half of these site-specific mismatches in small RNA sequences (Figure 2) were also present in full-length viral mRNA sequences assembled from RNA-seq data (Figure 3). Notably, these mismatches occur at relatively higher coverage regions (Figure 1). Specifically, loci editing A-to-G (transition) at 9048, 10967 and 14217; G-to-A (transition) at 2514, 4426 and 10848; G-to-C (transversion) at 4676 base positions. This suggests that there are some functional significance associated with the higher rates of small RNA production and subsequent modifications that are taking place at these loci. Most of these modifications occurring at higher coverage loci are also present in mRNA sequences (Figure 3) which suggest that these RNA modifications are the result of dsRNA editing. The most prevalent editing observed in this study was A-to-I editing which in higher metazoans is mediated by ADAR in dsRNA substrates (Savva et al., 2012). Although the exact mechanism for the occurrence of these mismatches in viral mRNA is not known, ADAR mediated RNA-editing is also common in both DNA and RNA viruses further ensuing proviral or antiviral effects (Gelinas et al., 2011). Additionally, during transcription of several RNA viruses, mRNAs are also subject to nucleotide(s) insertion unspecified by the viral genomes (Brennicke et al., 1999).

Table 2. Single base modification in 21-24 bases vsiRNA sequences produced by virus-infected gene-knockout mutants (Δ*ago*-2, Δ*dcl*-1 and Δ*dcl*-2) and wild-type (Vmicro) *Sclerotinia sclerotiorum*. Total mismatches for 12 possible nucleotide modifications are shown. Changes from reference bases to alternate bases are indicated by dot (.). Values within brackets are internal mismatches found in sequences of a given read size.

Samples	Read size	A.T	A.G	A.C	C.T	C.G	C.A	G.T	G.A	G.C	T.A	T.G	T.C
Ago2_SsHV2L (Replicate1)	18	88 (39)	270 (62)	38 (20)	163 (138)	7 (5)	55 (43)	97 (87)	249 (154)	37 (9)	49 (31)	36 (8)	140 (35)
	19	273 (166)	929 (277)	82 (57)	655 (560)	30 (29)	262 (229)	237 (217)	802 (469)	70 (30)	197 (133)	109 (22)	466 (115)
	20	804 (628)	2830 (606)	188 (102)	1870 (1564)	90 (74)	771 (668)	1077 (1036)	2429 (1458)	172 (89)	640 (429)	257 (71)	1292 (393)
	21	1969 (1608)	6703 (1472)	394 (238)	3555 (2957)	173 (127)	1663 (1345)	1961 (1790)	4738 (2634)	490 (210)	1715 (1208)	694 (190)	3177 (971)
	22	3496 (2789)	19039 (3369)	850 (511)	6967 (5606)	285 (214)	2630 (1974)	3079 (2762)	10913 (4086)	872 (231)	4011 (1973)	1698 (376)	8001 (2851)
	23	1636 (1239)	9359 (1378)	471 (274)	3814 (2939)	163 (102)	1384 (1082)	1546 (1369)	6539 (2803)	676 (142)	2050 (1083)	727 (230)	4915 (1278)
	24	687 (542)	1932 (480)	150 (98)	821 (608)	29 (16)	353 (299)	568 (506)	1532 (1090)	116 (62)	448 (204)	189 (51)	1162 (238)
Dcl1_SsHV2L (Replicate1)	18	57 (30)	317 (88)	49 (24)	226 (171)	17 (7)	63 (53)	47 (39)	256 (181)	42 (23)	75 (44)	84 (26)	303 (152)
	19	134 (97)	531 (136)	75 (23)	359 (279)	22 (11)	134 (119)	111 (96)	374 (242)	67 (38)	127 (89)	122 (55)	446 (223)
	20	282 (238)	919 (246)	113 (60)	646 (513)	35 (29)	333 (300)	510 (493)	821 (578)	139 (80)	281 (204)	179 (74)	588 (296)
	21	533 (451)	1377 (370)	198 (100)	975 (755)	87 (66)	620 (543)	631 (564)	1199 (834)	166 (72)	598 (472)	272 (124)	922 (438)
	22	919 (770)	2252 (574)	302 (148)	1378 (1006)	100 (71)	743 (670)	785 (718)	1645 (1041)	250 (103)	933 (748)	451 (166)	1297 (548)

	23	903 (749)	3043 (661)	312 (157)	1731 (1301)	108 (77)	841 (734)	1065 (998)	2236 (1382)	315 (98)	1054 (823)	469 (176)	1938 (766)
	24	809 (670)	1998 (484)	260 (117)	1214 (856)	95 (67)	667 (615)	847 (786)	1642 (1109)	185 (71)	630 (466)	325 (98)	1399 (510)
Dcl2_SsHV2L (Replicate1)	18	452 (357)	1619 (422)	250 (68)	1078 (784)	68 (51)	251 (197)	425 (399)	1344 (720)	89 (57)	221 (124)	169 (28)	790 (200)
	19	1548 (1303)	4441 (1200)	579 (184)	3355 (2528)	186 (135)	907 (786)	1226 (1118)	3790 (2112)	333 (166)	663 (433)	417 (94)	2151 (540)
	20	2866 (2233)	11950 (2697)	1404 (457)	8431 (6391)	419 (297)	2808 (2459)	4405 (4107)	11121 (6269)	825 (310)	2215 (1579)	1237 (250)	6208 (1270)
	21	7174 (5624)	33212 (8066)	4898 (1248)	17587 (12796)	910 (634)	5594 (4669)	7460 (6639)	28736 (11822)	2343 (1076)	5749 (3870)	3595 (669)	15527 (3512)
	22	16009 (11748)	107800 (18951)	9557 (2877)	44379 (30830)	2045 (1354)	10885 (8695)	17123 (15415)	59800 (26433)	6639 (1351)	11933 (7761)	12626 (1625)	48251 (12479)
	23	9255 (6743)	50138 (11707)	5092 (2027)	24273 (16392)	1065 (662)	5826 (4438)	8963 (7882)	37827 (17074)	5949 (853)	6284 (3544)	3526 (880)	28174 (5572)
	24	2575 (1868)	8385 (2150)	1050 (572)	3690 (2258)	253 (143)	992 (773)	2071 (1760)	6561 (4726)	591 (305)	1039 (551)	879 (185)	5383 (673)
Ago2_SsHV2L (Replicate2)	18	102 (61)	296 (64)	21 (2)	166 (131)	5 (4)	53 (36)	88 (81)	262 (154)	34 (5)	62 (42)	40 (12)	143 (40)
	19	321 (215)	857 (258)	90 (30)	655 (550)	32 (23)	295 (258)	264 (256)	813 (491)	127 (51)	226 (147)	127 (35)	444 (86)
	20	915 (751)	2766 (541)	202 (78)	2106 (1678)	80 (66)	957 (818)	1311 (1241)	2768 (1624)	311 (87)	828 (589)	311 (64)	1346 (344)
	21	2273 (1876)	6394 (1409)	451 (173)	3885 (3148)	162 (108)	2118 (1743)	2571 (2336)	5403 (2952)	720 (270)	2153 (1620)	724 (154)	3201 (935)
	22	4916 (3954)	18645 (2960)	860 (349)	7772 (5955)	333 (239)	3449 (2557)	4538 (4086)	12114 (5036)	1577 (279)	5006 (2709)	1977 (308)	8533 (2427)
	23	2015 (1583)	8601 (1275)	482 (230)	4042 (3049)	171 (107)	1825 (1481)	2019 (1794)	7076 (3147)	1026 (198)	2351 (1359)	596 (147)	4725 (1029)

	24	671 (560)	1122 (266)	107 (49)	719 (537)	54 (38)	291 (236)	540 (476)	1323 (953)	171 (71)	381 (225)	111 (29)	809 (121)
Dcl1_SsHV2L (Replicate2)	18	40 (29)	293 (65)	31 (6)	158 (89)	6 (4)	34 (29)	38 (32)	173 (109)	15 (13)	30 (13)	19 (2)	112 (43)
	19	109 (85)	692 (171)	88 (18)	365 (269)	26 (19)	135 (99)	116 (105)	471 (268)	56 (38)	104 (57)	48 (18)	355 (80)
	20	360 (281)	1866 (376)	193 (29)	1105 (815)	55 (42)	338 (272)	522 (485)	1454 (820)	119 (44)	291 (204)	148 (33)	924 (215)
	21	900 (707)	4792 (955)	689 (87)	2013 (1375)	83 (53)	761 (601)	925 (824)	3031 (1419)	308 (140)	740 (504)	410 (73)	2004 (576)
	22	1844 (1436)	14196 (1935)	994 (213)	4028 (2653)	143 (95)	1118 (828)	1988 (1790)	6378 (2589)	819 (186)	1570 (935)	1427 (151)	5419 (1427)
	23	700 (495)	4190 (765)	456 (145)	1875 (1241)	89 (49)	540 (416)	789 (702)	3719 (1365)	510 (113)	630 (311)	234 (62)	2656 (538)
	24	192 (146)	625 (184)	104 (28)	282 (172)	14 (8)	93 (68)	150 (127)	607 (437)	80 (41)	94 (51)	52 (20)	453 (81)
Dcl2_SsHV2L (Replicate2)	18	178 (136)	1068 (257)	121 (34)	547 (384)	29 (24)	106 (82)	224 (197)	800 (437)	35 (20)	115 (64)	77 (24)	420 (118)
	19	713 (586)	2896 (799)	363 (126)	1675 (1259)	98 (80)	533 (461)	649 (598)	2322 (1266)	216 (123)	347 (263)	233 (45)	1158 (278)
	20	1582 (1266)	7133 (1570)	739 (233)	4731 (3648)	301 (224)	1515 (1328)	2297 (2165)	6511 (3604)	555 (154)	1203 (879)	606 (153)	3404 (715)
	21	3854 (3141)	20138 (4938)	2681 (617)	9848 (7206)	532 (405)	3298 (2804)	4236 (3782)	16911 (6527)	1493 (651)	3054 (2154)	1591 (319)	8445 (1911)
	22	10150 (7704)	73942 (11991)	4818 (1526)	26779 (19032)	1328 (949)	6472 (5195)	11839 (10809)	39107 (16088)	4506 (967)	7259 (4896)	7163 (907)	29195 (7922)
	23	6058 (4582)	35421 (7840)	3020 (1181)	15384 (10485)	729 (459)	3695 (2935)	6037 (5411)	24761 (10862)	4339 (590)	3675 (2110)	1839 (524)	17558 (3419)
	24	1395 (1035)	5774 (1592)	595 (297)	2499 (1494)	190 (104)	726 (555)	1283 (1098)	4527 (3415)	368 (197)	515 (251)	489 (82)	3530 (393)

1Vmicro-type (Replicate1)	18	86 (68)	200 (27)	44 (24)	95 (45)	24 (8)	124 (82)	136 (115)	124 (57)	114 (33)	88 (56)	111 (24)	130 (28)
	19	257 (213)	559 (43)	103 (49)	229 (152)	47 (16)	280 (224)	256 (197)	255 (123)	216 (97)	280 (220)	246 (55)	316 (54)
	20	635 (498)	1596 (197)	194 (88)	656 (404)	99 (41)	767 (559)	727 (604)	795 (390)	434 (72)	610 (441)	1647 (90)	1729 (137)
	21	1328 (1016)	5895 (276)	689 (419)	1531 (724)	246 (69)	1777 (846)	1575 (1087)	3152 (1111)	1075 (213)	1727 (1114)	4500 (483)	2937 (551)
	22	2369 (1571)	11959 (892)	1306 (570)	2936 (1136)	558 (95)	3330 (1319)	2450 (1430)	5265 (1062)	2574 (281)	3579 (1898)	5267 (804)	24895 (1136)
	23	1334 (950)	4210 (326)	983 (450)	1552 (645)	359 (55)	1713 (815)	1637 (1048)	9947 (886)	1623 (190)	2148 (1130)	2216 (273)	2730 (473)
	24	601 (504)	813 (105)	373 (125)	521 (349)	120 (46)	515 (394)	771 (636)	1844 (1019)	627 (91)	515 (403)	511 (149)	399 (121)
2Vmicro (Replicate2)	18	52 (43)	163 (15)	21 (12)	48 (24)	6 (2)	98 (63)	67 (46)	83 (40)	108 (69)	47 (32)	68 (8)	67 (14)
	19	163 (152)	389 (26)	56 (20)	138 (94)	25 (13)	168 (133)	163 (130)	155 (93)	191 (135)	188 (141)	134 (13)	161 (25)
	20	420 (340)	918 (80)	111 (53)	371 (235)	54 (22)	468 (361)	467 (401)	452 (251)	228 (44)	417 (305)	713 (67)	856 (64)
	21	899 (730)	3018 (141)	342 (179)	883 (503)	118 (36)	1035 (553)	926 (703)	1535 (586)	629 (145)	1318 (862)	2562 (214)	1395 (216)
	22	1561 (1115)	6293 (453)	715 (278)	1813 (758)	340 (58)	2264 (901)	1587 (983)	2885 (687)	1631 (247)	2362 (1250)	3182 (392)	10058 (620)
	23	1026 (802)	3108 (261)	626 (283)	1062 (447)	245 (45)	1318 (642)	1070 (680)	4556 (612)	1055 (185)	1490 (791)	1479 (170)	1540 (223)
	24	356 (294)	524 (61)	242 (57)	323 (231)	90 (38)	380 (271)	505 (414)	1140 (746)	463 (81)	424 (333)	363 (112)	307 (86)

A.

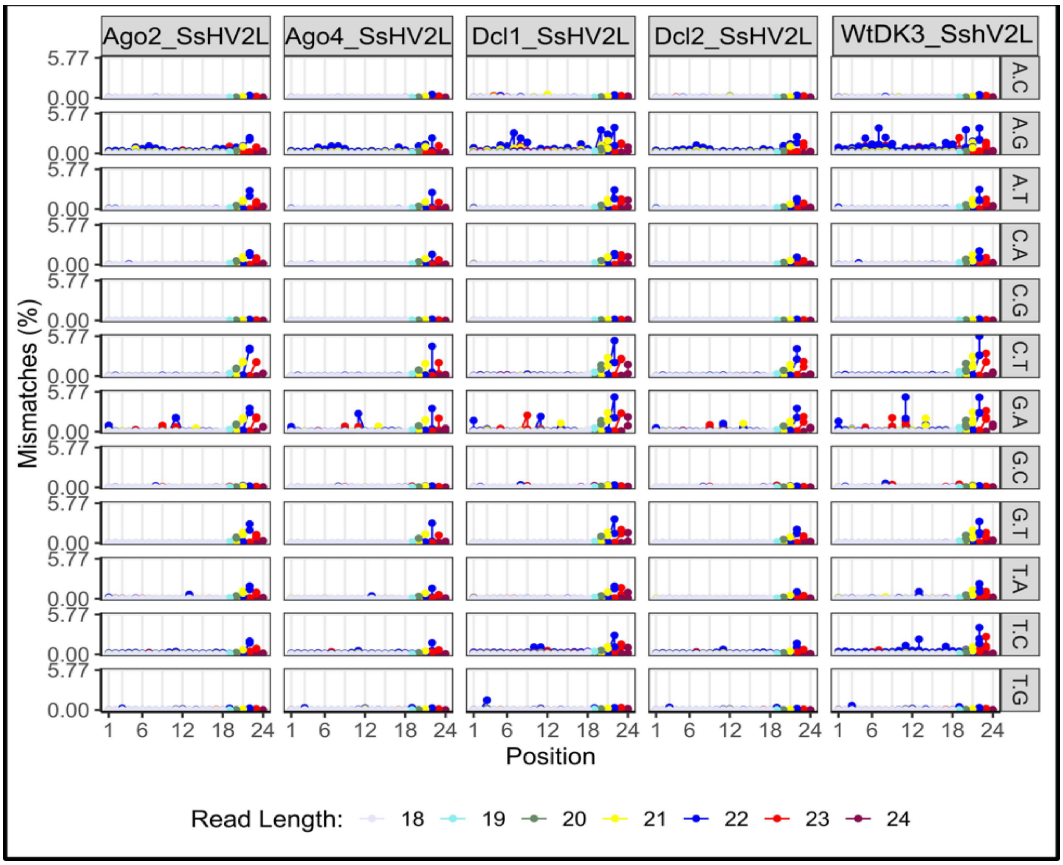
Ago2_SsHV2L
Ago4_SsHV2L
Dcl1_SsHV2L
Dcl2_SsHV2L
WtDK3_SshV2L
A.C
A.G
A.T
C.A
C.G
C.T
G.A
G.C
G.T
T.A
T.C
T.G
Mismatches (%)
5.77
0.00
1 6 12 18 24
Position
Read Length: 18 19 20 21 22 23 24

B.

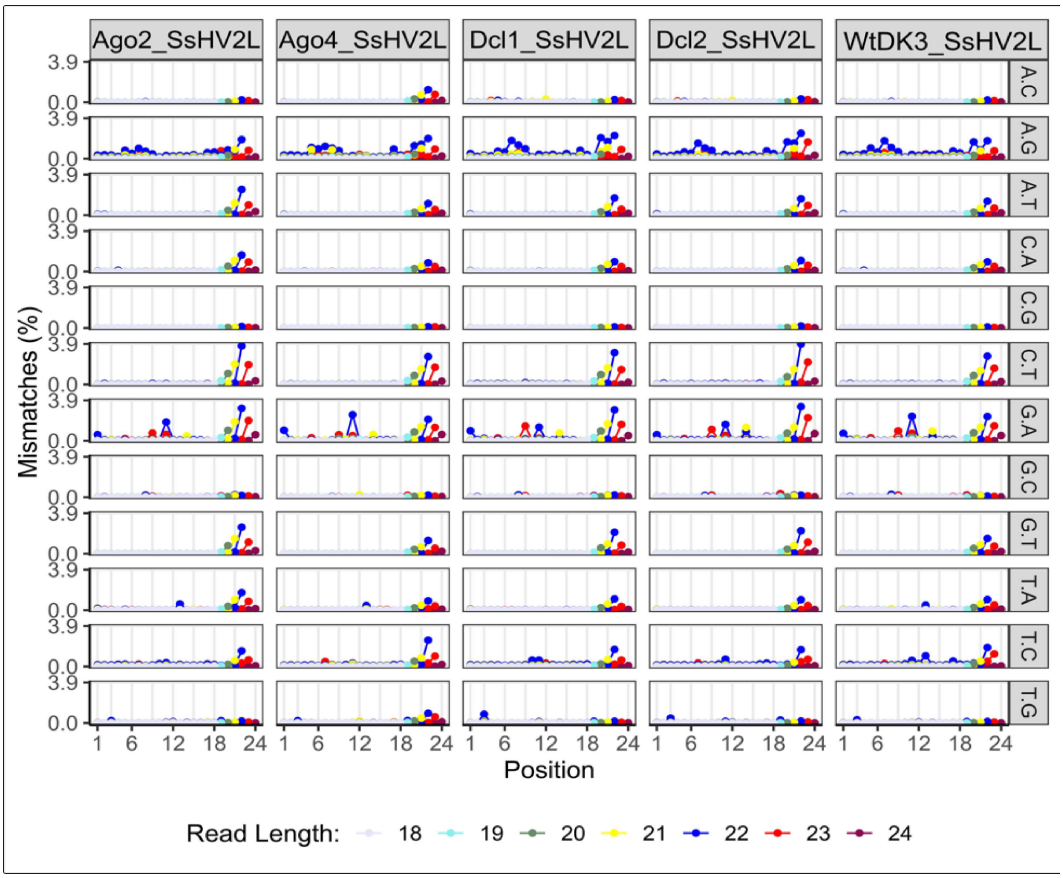
Ago2_SsHV2L
Ago4_SsHV2L
Dcl1_SsHV2L
Dcl2_SsHV2L
WtDK3_SsHV2L
A.C
A.G
A.T
C.A
C.G
C.T
G.A
G.C
G.T
T.A
T.C
T.G
Mismatches (%)
3.9
0.0
1 6 12 18 24
Position
Read Length: 18 19 20 21 22 23 24

Figure 1. Internal and terminal mismatches in vsiRNAs from both replicates, (**A**) replicate1 and (**B**) replicate2 of small RNA-seq datasets of *Sclerotinia sclerotiorum*. Mismatches (%) is the percentage of total RNA-editing events in each library.

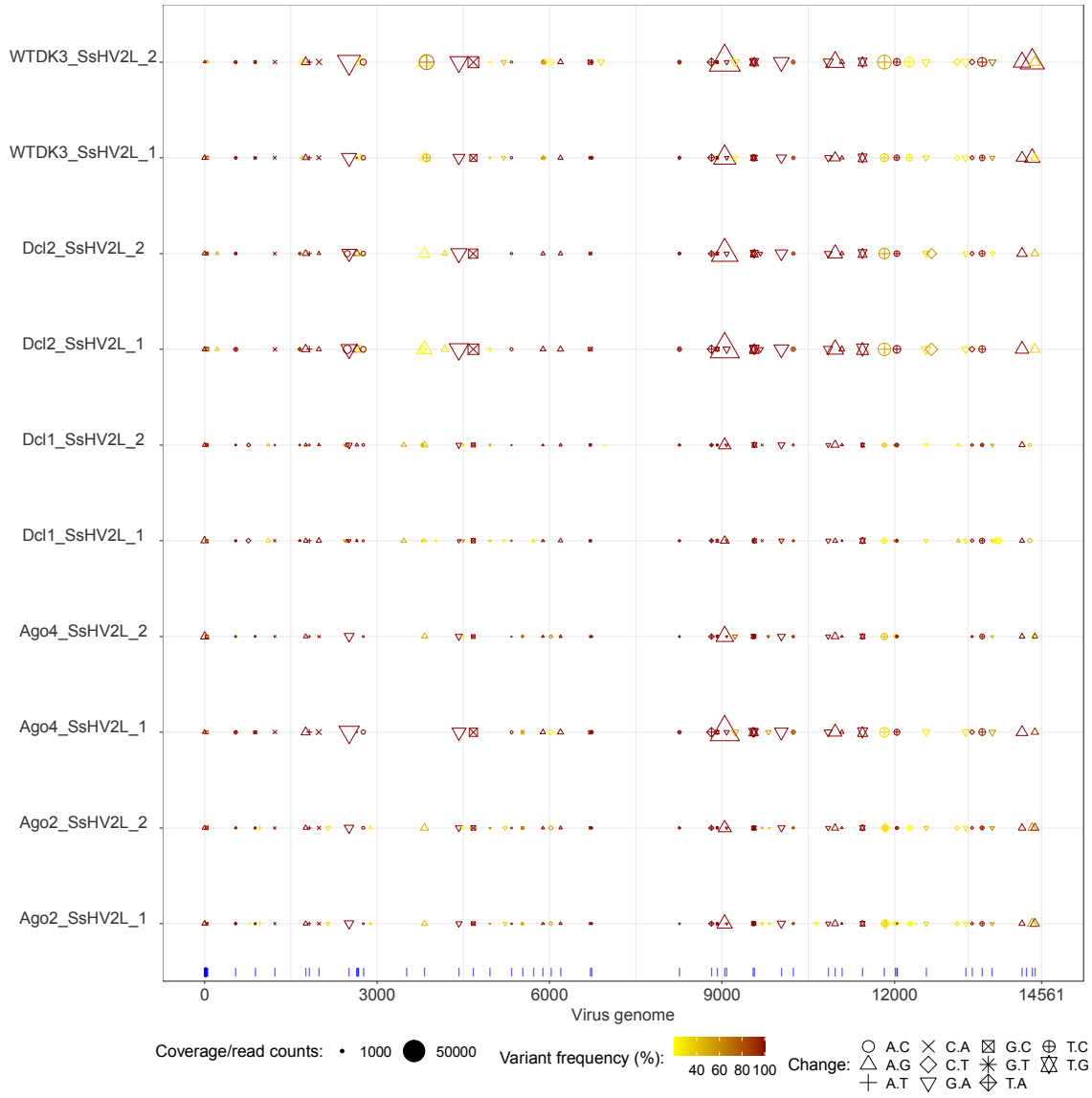

Figure 2. Single Nucleotide Polymorphism (SNP) sites in small RNA libraries. Small RNA reads were aligned to Sclerotinia sclerotiorum hypovirus 2 L (SsHV2-L) genome. Coverage represents the total number of reads and variant frequency represents the percentage of mismatches present at any given base position. Variant sites with more than 20X coverage and 20% frequency are shown. Internal ticks (blue-colored) on X-axis represent the SNP sites that are present in both small RNA and RNA-seq libraries.

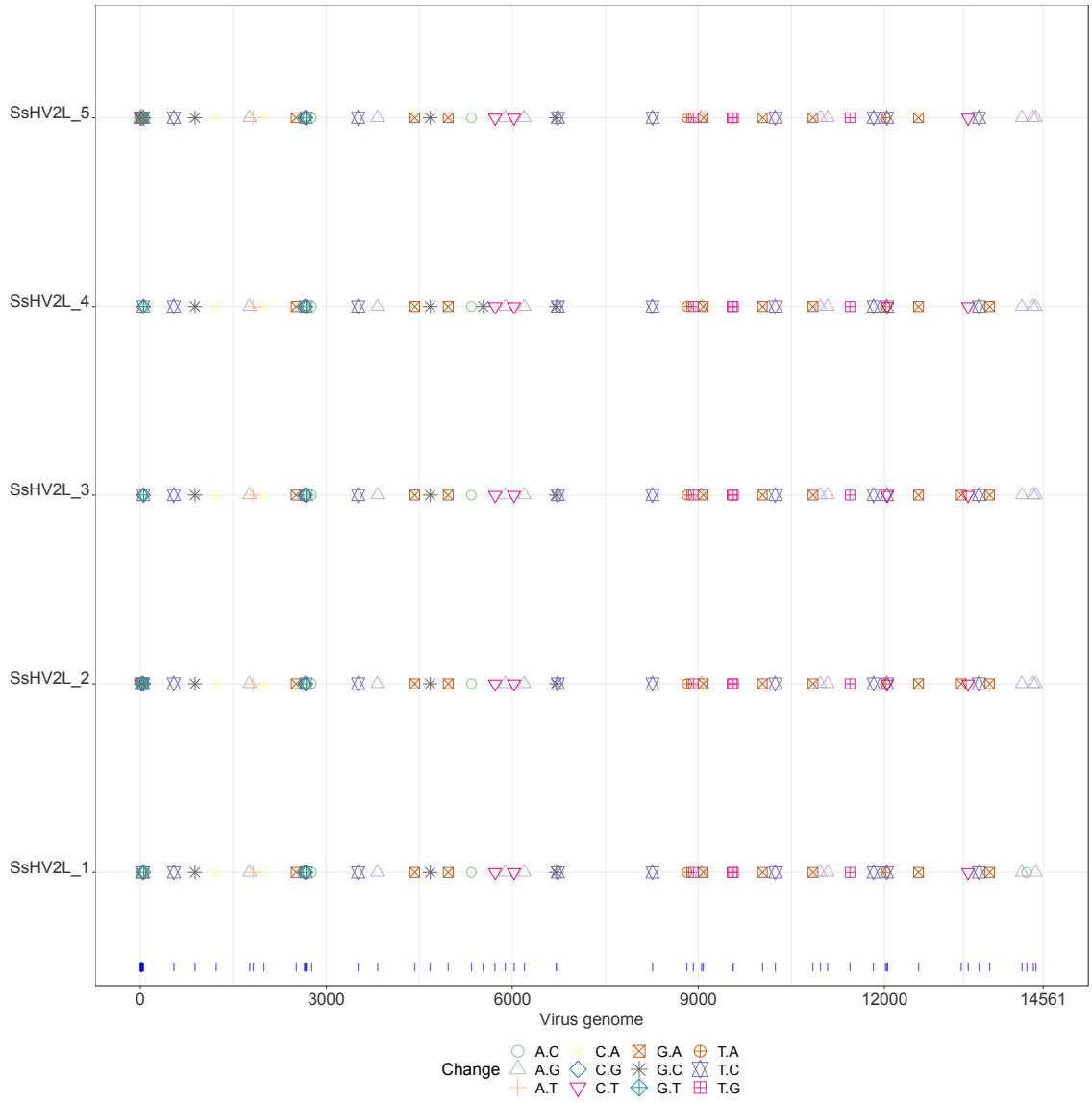

Figure 3. Single Nucleotide Polymorphism (SNP) sites from five RNA-seq libraries of wild-type *Sclerotinia sclerotiorum* infected with Sclerotinia sclerotiorum hypovirus 2 L (SsHV2-L) virus. Full-length, assembled contigs were aligned to the virus genome. Internal ticks (blue-colored) on X-axis represent the SNP sites that are present in both small RNA and RNA-seq libraries.

1.5.2 Virus-derived small RNAs in other fungi: *Botrytis cinerea* and *Fusarium graminearum*

Small RNA data from closely related fungal species, such as *Botrytis* and *Fusarium* spp. were also analyzed from publicly available datasets. In *B. cinerea*, similar modification of vsiRNA sequences were observed. *Botrytis cinerea* isolates, Pi285.8 (infected with *Narnavirus* and *Mitovirus*), v446 (infected with unclassified viruses) and v448 (infected with *Mitovirus*, *Flexivirus* and unclassified viruses) all showed similar patterns of RNA-editing with both internal and terminal modifications (Table 3). Apart from terminal modifications, several internal edit sites were found in *B. cinerea* modifying A-to-C at 1st, 8th, and 15th base of 21 bases; and T-to-A and T-to-G at the 1st base of 21 bases long vsiRNAs (Figure 4A-C).

RNA-editing with both internal and terminal modifications were also present in a model filamentous fungus, *F. graminearum*. While terminal modifications were present in all sequence size, internal modifications in *F. graminearum* were primarily found in 22 bases long vsiRNAs, specifically for T-to-C change at the 8th and 13th bases; and C-to-G change at 10th base (Figure 4D). Additionally, these three fungal species compared in this study showed prevalence for size-specific internal modifications of vsiRNA: *S. sclerotiorum* in 18, 22 and 23 bases long sequences, *B. cinerea* in 21 bases long sequences and *F. graminearum* primarily in 22 bases long sequences.

Another interesting aspect to consider is the abundance of vsiRNAs production in each of these species. For example, vsiRNAs produced (in terms of percentage) by *S. sclerotiorum* and *F. graminearum* is relatively higher than *B. cinerea* (Table 1 and Table 3). One hypothesis to support this difference is that the biogenesis of vsiRNAs is directly correlated with the host susceptibility, virus suppressor of RNA silencing (VSR) activity,

and pathogenicity of each infecting virus. This is well illustrated in plants. Under limiting environmental conditions such as low temperature, pathways involved in vsiRNAs production is hindered, and consequently the RNA silencing defense machinery is disrupted (Szittya et al., 2003). As a result, viruses lacking in VSR activity can infect plants only in low temperatures (Szittya et al., 2003).

Table 3. Incidence of RNA-editing in 21-24 bases vsiRNA sequences produced by virus-infected *Botrytis*, *Fusarium*, human and mouse samples. Total vsiRNAs, mismatches and mismatch % (of total vsiRNAs) are shown.

Organism	**Isolates/ Cell lines**	**Infection**	**VsiRNAs (% of library)**	**SRA (accessions)**	**Mismatches**					
					Terminal	**Internal**	**Total**	**Terminal %**	**Internal %**	**Total %**
Botrytis cinerea	Pi285.8	numerous	635951 (5.07%)	SRR3659825	12324	18177	30501	1.94	2.86	4.80
	V446	numerous	229493 (2.47%)	SRR3659826	4395	7861	12256	1.92	3.43	5.34
	V448	numerous	868052 (7.16%)	SRR3659827	25324	33033	58357	2.92	3.81	6.72
Fusarium graminearum		HV1	2418724 (21.11%)	SRR3055827	77862	288669	366531	3.22	11.93	15.15
Human	293T cells	*Enterovirus* (HEV71)-WT	65833 (0.23%)	SRR5593145	1862	1613	3475	2.83	2.45	5.28
	293T cells	*Enterovirus* (HEV71)-D23A	1081903 (3.58%)	SRR5593146	112217	74690	186907	10.37	6.90	17.28
	293T cells	*Enterovirus* (HEV71)-D23A	1339758 (5.27%)	SRR5593147	163117	90336	253453	12.18	6.74	18.92
	Dicer-deficient 293T	*Enterovirus* (HEV71)-D23A	4318 (0.01%)	SRR5593148	100	122	222	2.32	2.83	5.14
Mouse	BALB/c	*Nodamura* (2dp1)	59387 (0.40%)	SRR2175652	17549	7357	24906	29.55	12.39	41.94
	BALB/c	*Nodamura* (1dpi)	15199 (0.11%)	SRR2175613	1057	1718	2775	6.95	11.30	18.26
	BALB/c	*Nodamura* (4dpi)	2134229 (15.37%)	SRR2175618	20331	227659	247990	0.95	10.67	11.62

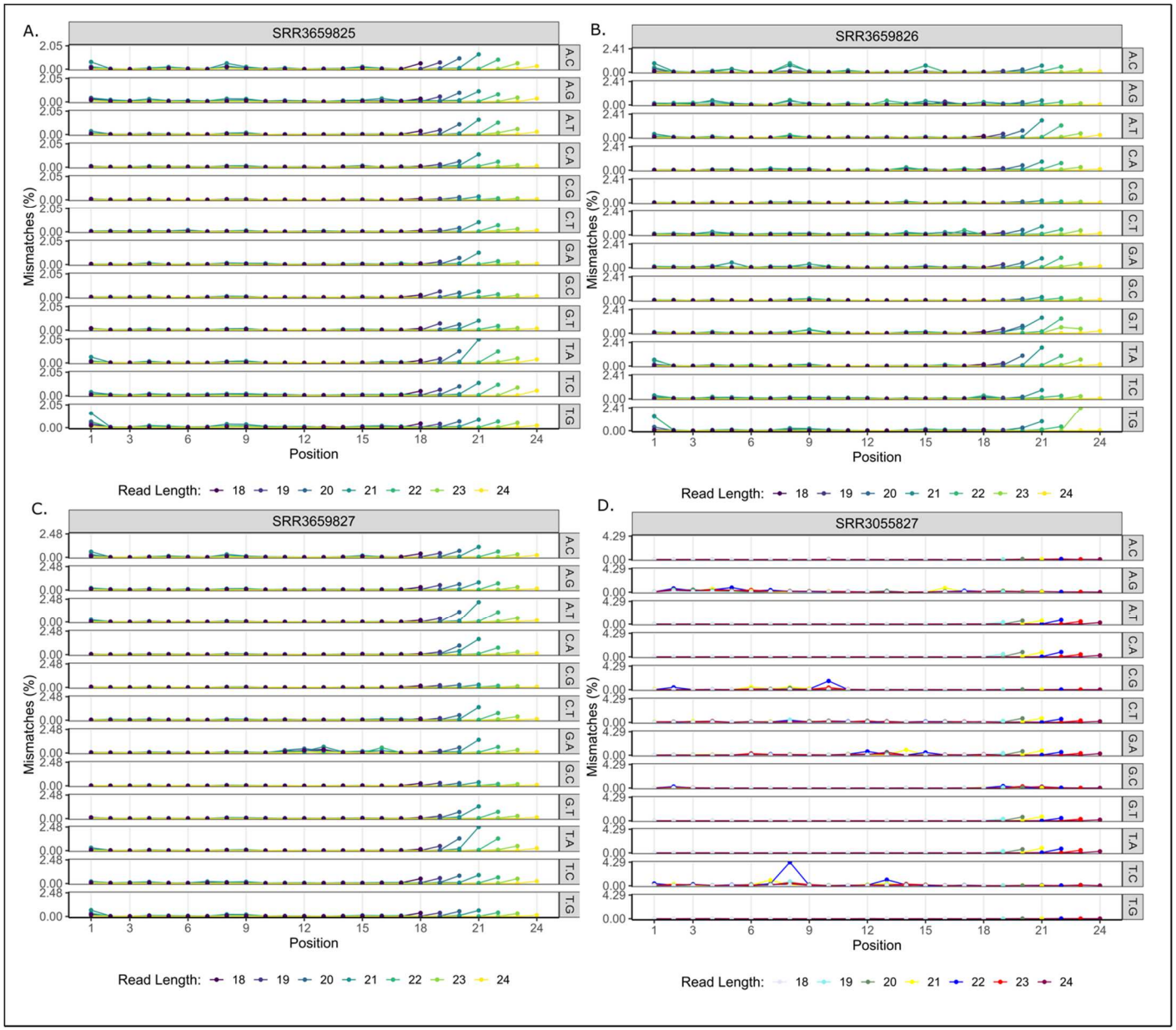
A.
SRR3659825
B.
SRR3659826
C.
SRR3659827
D.
SRR3055827
Mismatches (%)
Position
A.C
A.G
A.T
C.A
C.G
C.T
G.A
G.C
G.T
T.A
T.C
T.G
Read Length: 18 19 20 21 22 23 24

Figure 4. Internal and terminal mismatches in vsiRNA produced by three isolates, (**A.**)Pi285.8 (infected with Narnavirus and Mitovirus), (**B.**) v446 (infected with unclassified viruses) and (**C.**) v448 (infected with Mitovirus, Flexivirus and unclassified viruses) of *Botrytis cinerea*. (**D.**) Internal and terminal mismatches in vsiRNA produced by *Fusarium graminearum* infected with Fusarium graminearum hypovirus 1 (FgHV1). Mismatches % is the percentage of total RNA-editing events in each library.

1.5.3 Virus-derived small RNAs in mouse and human

To further investigate the prevalence of editing events in vsiRNAs produced by higher metazoans, mouse and human small RNA-seq data were analyzed. In mammals, biogenesis of vsiRNA is associated with the antiviral immunity (Qiu et al., 2017). Human data (Qiu et al., 2017) analyzed in this study also show clear role of dicer in antiviral immunity through biogenesis of vsiRNAs (Table 3). Human enterovirus 71 (HEV71) 3A protein is a viral suppressor of RNAi and viral infection with HEV 71 is affected with the biogenesis of vsiRNAs (Qiu et al., 2017). Biogenesis of vsiRNAs is inhibited in no-dicer cell lines even when infected with VSR deficient HEV71 (Table 3). In mouse, virus-derived small RNAs were produced in relatively low number until 4 days post inoculation (dpi) with *Nodamura* virus (Table 3). Although both internal and terminal modifications were found in mouse vsiRNAs, only terminal modifications were found in vsiRNAs from human (Figure 5). In mouse, C-to-A and G-to-T internal modifications were found at the 1st and 4th bases of 21, 22 and 23 nucleotide long sequences.

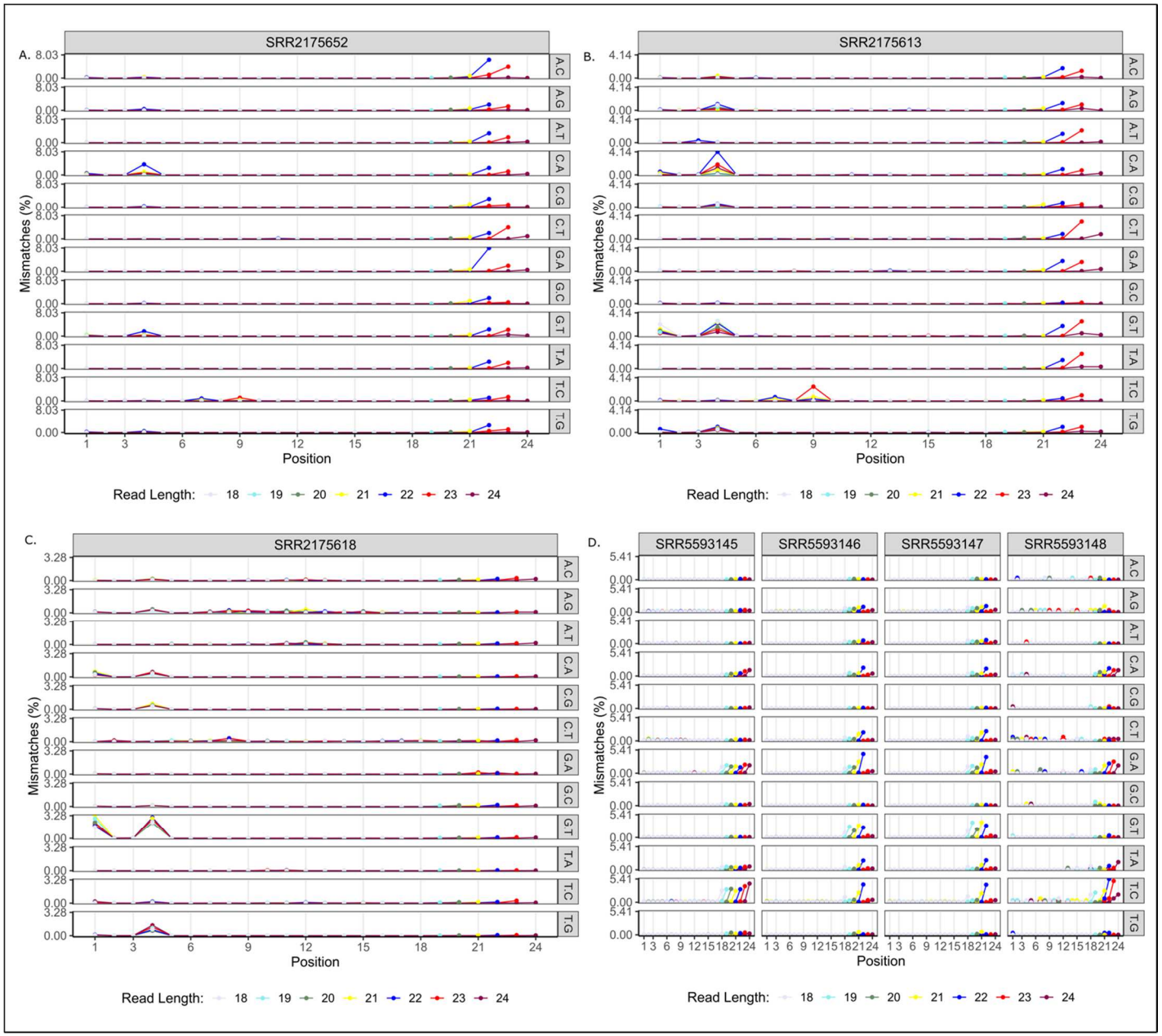
A.
SRR2175652
B.
SRR2175613
C.
SRR2175618
D.
SRR5593145
SRR5593146
SRR5593147
SRR5593148
Mismatches (%)
Position
A.C
A.G
A.T
C.A
C.G
C.T
G.A
G.C
G.T
T.A
T.C
T.G
Read Length: 18 19 20 21 22 23 24

Figure 5. (**A-C.**) Internal and terminal mismatches in vsiRNA produced by mouse (BALB/c). (**D.**) Internal and terminal mismatches in vsiRNA produced by human 293T cells infected with *Enterovirus* (details in Table 3). Mismatches % is the percentage of total RNA-editing events in each library.

Considering the abundance of both internal and terminal mismatches in vsiRNAs, there is a possibility of several independently established mechanisms of RNA-editing associated with vsiRNAs and viral mRNAs. Since RNA-editing is an evolutionarily conserved mechanism, cross-species study of these editing sites and elucidating their biological roles are important to better understand antiviral RNA silencing and the exploration as antiviral therapeutics.

References

Aliyari, R., and Ding, S.W. (2009). RNA-based viral immunity initiated by the Dicer family of host immune receptors. *Immunol Rev* 227**,** 176-188.

Amselem, J., Cuomo, C.A., Van Kan, J.A., Viaud, M., Benito, E.P., Couloux, A., Coutinho, P.M., De Vries, R.P., Dyer, P.S., Fillinger, S., Fournier, E., Gout, L., Hahn, M., Kohn, L., Lapalu, N., Plummer, K.M., Pradier, J.M., Quevillon, E., Sharon, A., Simon, A., Ten Have, A., Tudzynski, B., Tudzynski, P., Wincker, P., Andrew, M., Anthouard, V., Beever, R.E., Beffa, R., Benoit, I., Bouzid, O., Brault, B., Chen, Z., Choquer, M., Collemare, J., Cotton, P., Danchin, E.G., Da Silva, C., Gautier, A., Giraud, C., Giraud, T., Gonzalez, C., Grossetete, S., Guldener, U., Henrissat, B., Howlett, B.J., Kodira, C., Kretschmer, M., Lappartient, A., Leroch, M., Levis, C., Mauceli, E., Neuveglise, C., Oeser, B., Pearson, M., Poulain, J., Poussereau, N., Quesneville, H., Rascle, C., Schumacher, J., Segurens, B., Sexton, A., Silva, E., Sirven, C., Soanes, D.M., Talbot, N.J., Templeton, M., Yandava, C., Yarden, O., Zeng, Q., Rollins, J.A., Lebrun, M.H., and Dickman, M. (2011). Genomic analysis of the necrotrophic fungal pathogens Sclerotinia sclerotiorum and Botrytis cinerea. *PLoS Genet* 7**,** e1002230.

Axtell, M.J. (2013). ShortStack: comprehensive annotation and quantification of small RNA genes. *Rna*.

Basilio, C., Wahba, A.J., Lengyel, P., Speyer, J.F., and Ochoa, S. (1962). Synthetic polynucleotides and the amino acid code. V. *Proc Natl Acad Sci U S A* 48**,** 613-616.

Baulcombe, D. (2002). Viral suppression of systemic silencing. *Trends in Microbiology* 10**,** 306-308.

Baulcombe, D. (2004). RNA silencing in plants. *Nature* 431**,** 356-363.

Baulcombe, D. (2005). RNA silencing. *Trends Biochem Sci* 30**,** 290-293.

Benne, R., Van Den Burg, J., Brakenhoff, J.P., Sloof, P., Van Boom, J.H., and Tromp, M.C. (1986). Major transcript of the frameshifted coxII gene from trypanosome mitochondria contains four nucleotides that are not encoded in the DNA. *Cell* 46**,** 819-826.

Bernstein, E., Caudy, A.A., Hammond, S.M., and Hannon, G.J. (2001). Role for a bidentate ribonuclease in the initiation step of RNA interference. *Nature* 409**,** 363-366.

Bouche, N., Lauressergues, D., Gasciolli, V., and Vaucheret, H. (2006). An antagonistic function for Arabidopsis DCL2 in development and a new function for DCL4 in generating viral siRNAs. *EMBO J* 25**,** 3347-3356.

Brennicke, A., Marchfelder, A., and Binder, S. (1999). RNA editing. *FEMS Microbiology Reviews* 23**,** 297-316.

Bushnell, B. (2014). "BBMap: a fast, accurate, splice-aware aligner". Lawrence Berkeley National Lab.(LBNL), Berkeley, CA (United States)).

Catalanotto, C., Azzalin, G., Macino, G., and Cogoni, C. (2002). Involvement of small RNAs and role of the qde genes in the gene silencing pathway in Neurospora. *Genes Dev* 16**,** 790-795.

Catalanotto, C., Pallotta, M., Refalo, P., Sachs, M.S., Vayssie, L., Macino, G., and Cogoni, C. (2004). Redundancy of the two dicer genes in transgene-induced

posttranscriptional gene silencing in Neurospora crassa. *Mol Cell Biol* 24**,** 2536-2545.

Dang, Y., Yang, Q., Xue, Z., and Liu, Y. (2011). RNA interference in fungi: pathways, functions, and applications. *Eukaryot Cell* 10**,** 1148-1155.

Deleris, A., Gallego-Bartolome, J., Bao, J., Kasschau, K.D., Carrington, J.C., and Voinnet, O. (2006). Hierarchical action and inhibition of plant Dicer-like proteins in antiviral defense. *Science* 313**,** 68-71.

Ding, S.W., and Voinnet, O. (2007). Antiviral immunity directed by small RNAs. *Cell* 130**,** 413-426.

Donaire, L., and Ayllon, M.A. (2017). Deep sequencing of mycovirus-derived small RNAs from Botrytis species. *Mol Plant Pathol* 18**,** 1127-1137.

Dunoyer, P., Himber, C., and Voinnet, O. (2005). DICER-LIKE 4 is required for RNA interference and produces the 21-nucleotide small interfering RNA component of the plant cell-to-cell silencing signal. *Nat Genet* 37**,** 1356-1360.

Elbashir, S.M., Lendeckel, W., and Tuschl, T. (2001). RNA interference is mediated by 21-and 22-nucleotide RNAs. *Genes & Development* 15**,** 188-200.

Fire, A., Xu, S.Q., Montgomery, M.K., Kostas, S.A., Driver, S.E., and Mello, C.C. (1998). Potent and specific genetic interference by double-stranded RNA in Caenorhabditis elegans. *Nature* 391**,** 806-811.

Gelinas, J.F., Clerzius, G., Shaw, E., and Gatignol, A. (2011). Enhancement of replication of RNA viruses by ADAR1 via RNA editing and inhibition of RNA-activated protein kinase. *J Virol* 85**,** 8460-8466.

Gerber, A.P., and Keller, W. (2001). RNA editing by base deamination: more enzymes, more targets, new mysteries. *Trends Biochem Sci* 26**,** 376-384.

Grabherr, M.G., Haas, B.J., Yassour, M., Levin, J.Z., Thompson, D.A., Amit, I., Adiconis, X., Fan, L., Raychowdhury, R., Zeng, Q., Chen, Z., Mauceli, E., Hacohen, N., Gnirke, A., Rhind, N., Di Palma, F., Birren, B.W., Nusbaum, C., Lindblad-Toh, K., Friedman, N., and Regev, A. (2011). Full-length transcriptome assembly from RNA-Seq data without a reference genome. *Nat Biotechnol* 29**,** 644-652.

Hamilton, A., Voinnet, O., Chappell, L., and Baulcombe, D. (2002). Two classes of short interfering RNA in RNA silencing. *Embo Journal* 21**,** 4671-4679.

Hamilton, A.J., and Baulcombe, D.C. (1999). A species of small antisense RNA in posttranscriptional gene silencing in plants. *Science* 286**,** 950-952.

Hammond, T.M., and Keller, N.P. (2005). RNA silencing in Aspergillus nidulans is independent of RNA-dependent RNA polymerases. *Genetics* 169**,** 607-617.

Heffer Link, V., and Johnson, K. (2007). "White mold. The plant health instructor. doi: 10.1094". PHI-I-2007-0809-01).

Hock, J., and Meister, G. (2008). The Argonaute protein family. *Genome Biol* 9**,** 210.

Jin, Y.F., Zhang, W.J., and Li, Q. (2009). Origins and Evolution of ADAR-mediated RNA Editing. *Iubmb Life* 61**,** 572-578.

Kadotani, N., Nakayashiki, H., Tosa, Y., and Mayama, S. (2003). RNA silencing in the phytopathogenic fungus Magnaporthe oryzae. *Mol Plant Microbe Interact* 16**,** 769-776.

Kallman, A.M., Sahlin, M., and Ohman, M. (2003). ADAR2 A-->I editing: site selectivity and editing efficiency are separate events. *Nucleic Acids Res* 31**,** 4874-4881.

Khvorova, A., Reynolds, A., and Jayasena, S.D. (2003). Functional siRNAs and miRNAs exhibit strand bias. *Cell* 115**,** 209-216.

Langmead, B., Trapnell, C., Pop, M., and Salzberg, S.L. (2009). Ultrafast and memory-efficient alignment of short DNA sequences to the human genome. *Genome Biol* 10**,** R25.

Laurie, J.D., Ali, S., Linning, R., Mannhaupt, G., Wong, P., Guldener, U., Munsterkotter, M., Moore, R., Kahmann, R., Bakkeren, G., and Schirawski, J. (2012). Genome Comparison of Barley and Maize Smut Fungi Reveals Targeted Loss of RNA Silencing Components and Species-Specific Presence of Transposable Elements. *Plant Cell* 24**,** 1733-1745.

Lee Marzano, S.Y., Neupane, A., and Domier, L. (2018). Transcriptional and Small RNA Responses of the White Mold Fungus Sclerotinia sclerotiorum to Infection by a Virulence-Attenuating Hypovirus. *Viruses-Basel* 10.

Lerner, T., Papavasiliou, F.N., and Pecori, R. (2018). RNA Editors, Cofactors, and mRNA Targets: An Overview of the C-to-U RNA Editing Machinery and Its Implication in Human Disease. *Genes (Basel)* 10.

Li, Y., Lu, J., Han, Y., Fan, X., and Ding, S.W. (2013). RNA interference functions as an antiviral immunity mechanism in mammals. *Science* 342**,** 231-234.

Liu, H., Li, Y., Chen, D., Qi, Z., Wang, Q., Wang, J., Jiang, C., and Xu, J.R. (2017). A-to-I RNA editing is developmentally regulated and generally adaptive for sexual reproduction in Neurospora crassa. *Proc Natl Acad Sci U S A* 114**,** E7756-e7765.

Liu, H., Wang, Q., He, Y., Chen, L., Hao, C., Jiang, C., Li, Y., Dai, Y., Kang, Z., and Xu, J.R. (2016). Genome-wide A-to-I RNA editing in fungi independent of ADAR enzymes. *Genome Res* 26**,** 499-509.

Mahendran, R., Spottswood, M.R., and Miller, D.L. (1991). RNA editing by cytidine insertion in mitochondria of Physarum polycephalum. *Nature* 349**,** 434-438.

Mochama, P., Jadhav, P., Neupane, A., and Lee Marzano, S.Y. (2018). Mycoviruses as Triggers and Targets of RNA Silencing in White Mold Fungus Sclerotinia sclerotiorum. *Viruses* 10.

Nakayashiki, H., Kadotani, N., and Mayama, S. (2006). Evolution and diversification of RNA silencing proteins in fungi. *J Mol Evol* 63**,** 127-135.

Navaratnam, N., Fujino, T., Bayliss, J., Jarmuz, A., How, A., Richardson, N., Somasekaram, A., Bhattacharya, S., Carter, C., and Scott, J. (1998). Escherichia coli cytidine deaminase provides a molecular model for ApoB RNA editing and a mechanism for RNA substrate recognition. *J Mol Biol* 275**,** 695-714.

Navaratnam, N., Morrison, J.R., Bhattacharya, S., Patel, D., Funahashi, T., Giannoni, F., Teng, B.B., Davidson, N.O., and Scott, J. (1993). The p27 catalytic subunit of the apolipoprotein B mRNA editing enzyme is a cytidine deaminase. *Journal of Biological Chemistry* 268**,** 20709-20712.

Neupane, A., Feng, C., Mochama, P.K., Saleem, H., and Lee Marzano, S.Y. (2019). Roles of Argonautes and Dicers on Sclerotinia sclerotiorum Antiviral RNA Silencing. *Front Plant Sci* 10**,** 976.

Nishikura, K. (2010). Functions and regulation of RNA editing by ADAR deaminases. *Annu Rev Biochem* 79**,** 321-349.

Nuss, D.L. (2005). Hypovirulence: Mycoviruses at the fungal-plant interface. *Nature Reviews Microbiology* 3**,** 632-642.

Pearson, M.N., Beever, R.E., Boine, B., and Arthur, K. (2009). Mycoviruses of filamentous fungi and their relevance to plant pathology. *Mol Plant Pathol* 10**,** 115-128.

Polson, A.G., and Bass, B.L. (1994). Preferential selection of adenosines for modification by double-stranded RNA adenosine deaminase. *EMBO J* 13**,** 5701-5711.

Qiu, Y., Xu, Y., Zhang, Y., Zhou, H., Deng, Y.Q., Li, X.F., Miao, M., Zhang, Q., Zhong, B., Hu, Y., Zhang, F.C., Wu, L., Qin, C.F., and Zhou, X. (2017). Human Virus-Derived Small RNAs Can Confer Antiviral Immunity in Mammals. *Immunity* 46**,** 992-1004.e1005.

Salk, J.J., Schmitt, M.W., and Loeb, L.A. (2018). Enhancing the accuracy of next-generation sequencing for detecting rare and subclonal mutations. *Nat Rev Genet* 19**,** 269-285.

Savva, Y.A., Rieder, L.E., and Reenan, R.A. (2012). The ADAR protein family. *Genome Biol* 13**,** 252.

Schwarz, D.S., Hutvagner, G., Du, T., Xu, Z., Aronin, N., and Zamore, P.D. (2003). Asymmetry in the assembly of the RNAi enzyme complex. *Cell* 115**,** 199-208.

Segers, G.C., Zhang, X., Deng, F., Sun, Q., and Nuss, D.L. (2007). Evidence that RNA silencing functions as an antiviral defense mechanism in fungi. *Proc Natl Acad Sci U S A* 104**,** 12902-12906.

Shi, Y., Yang, D.H., Xiong, J., Jia, J., Huang, B., and Jin, Y.X. (2005). Inhibition of genes expression of SARS coronavirus by synthetic small interfering RNAs. *Cell Res* 15**,** 193-200.

Sikhakolli, U.R., Lopez-Giraldez, F., Li, N., Common, R., Townsend, J.P., and Trail, F. (2012). Transcriptome analyses during fruiting body formation in Fusarium graminearum and Fusarium verticillioides reflect species life history and ecology. *Fungal Genet Biol* 49**,** 663-673.

Suzuki, N., Maruyama, K., Moriyama, M., and Nuss, D.L. (2003). Hypovirus papain-like protease p29 functions in trans to enhance viral double-stranded RNA accumulation and vertical transmission. *J Virol* 77**,** 11697-11707.

Szittya, G., Silhavy, D., Molnar, A., Havelda, Z., Lovas, A., Lakatos, L., Banfalvi, Z., and Burgyan, J. (2003). Low temperature inhibits RNA silencing-mediated defence by the control of siRNA generation. *EMBO J* 22**,** 633-640.

Teng, B., Burant, C.F., and Davidson, N.O. (1993). Molecular cloning of an apolipoprotein B messenger RNA editing protein. *Science* 260**,** 1816-1819.

Wang, M., Weiberg, A., Lin, F.-M., Thomma, B.P.H.J., Huang, H.-D., and Jin, H. (2016a). Bidirectional cross-kingdom RNAi and fungal uptake of external RNAs confer plant protection. *Nature Plants* 2**,** 16151.

Wang, S., Li, P., Zhang, J., Qiu, D., and Guo, L. (2016b). Generation of a high resolution map of sRNAs from Fusarium graminearum and analysis of responses to viral infection. *Sci Rep* 6**,** 26151.

Wang, Z., Lopez-Giraldez, F., Lehr, N., Farre, M., Common, R., Trail, F., and Townsend, J.P. (2014). Global gene expression and focused knockout analysis reveals genes

associated with fungal fruiting body development in Neurospora crassa. *Eukaryot Cell* 13**,** 154-169.

Wassenegger, M., and Krczal, G. (2006). Nomenclature and functions of RNA-directed RNA polymerases. *Trends Plant Sci* 11**,** 142-151.

Wolf, J., Gerber, A.P., and Keller, W. (2002). tadA, an essential tRNA-specific adenosine deaminase from Escherichia coli. *Embo Journal* 21**,** 3841-3851.

Wong, S.K., Sato, S., and Lazinski, D.W. (2001). Substrate recognition by ADAR1 and ADAR2. *RNA* 7**,** 846-858.

Zamore, P.D. (2001). RNA interference: listening to the sound of silence. *Nat Struct Biol* 8**,** 746-750.

Zamore, P.D. (2002). Ancient pathways programmed by small RNAs. *Science* 296**,** 1265-1269.

Zhang, C., Wu, Z., Li, Y., and Wu, J. (2015). Biogenesis, Function, and Applications of Virus-Derived Small RNAs in Plants. *Front Microbiol* 6**,** 1237.

Zhu, H., and Guo, H. (2012). The role of virus-derived small interfering RNAs in RNA silencing in plants. *Sci China Life Sci* 55**,** 119-125.

Zhu, Y., Luo, H., Zhang, X., Song, J., Sun, C., Ji, A., Xu, J., and Chen, S. (2014). Abundant and selective RNA-editing events in the medicinal mushroom Ganoderma lucidum. *Genetics* 196**,** 1047-1057.

CHAPTER TWO: METATRANSCRIPTOMIC ANALYSIS AND IN SILICO APPROACH IDENTIFIED MYCOVIRUSES IN THE ARBUSCULAR MYCORRHIZAL FUNGUS *RHIZOPHAGUS* SPP.

This chapter has been published in the journal *Viruses*:

Neupane, A., Feng, C., Feng, J., Kafle, A., Bucking, H., and Lee Marzano, S.Y. (2018). Metatranscriptomic Analysis and In Silico Approach Identified Mycoviruses in the Arbuscular Mycorrhizal Fungus *Rhizophagus* spp. Viruses 10

Abstract

Arbuscular mycorrhizal fungi (AMF), including *Rhizophagus* spp., can play important roles in nutrient cycling of the rhizosphere. However, the effect of virus infection on AMF's role in nutrient cycling cannot be determined without first knowing the diversity of the mycoviruses in AMF. Therefore, in this study, we sequenced the *R. irregularis* isolate-09 due to its previously demonstrated high efficiency in increasing the N/P uptake of the plant. We identified one novel mitovirus contig of 3685 bp, further confirmed by reverse transcription-PCR. Also, publicly available *Rhizophagus* spp. RNA-Seq data were analyzed to recover five partial virus sequences from family *Narnaviridae*, among which four were from *R. diaphanum* MUCL-43196 and one was from *R. irregularis* strain-C2 that was similar to members of the *Mitovirus* genus. These contigs coded genomes larger than the regular mitoviruses infecting pathogenic fungi and can be translated by either a mitochondrial translation code or a cytoplasmic translation code, which was also reported in previously found mitoviruses infecting mycorrhizae. The five newly identified virus sequences are comprised of functionally conserved RdRp motifs and formed two separate subclades with mitoviruses infecting *Gigaspora margarita* and *Rhizophagus clarus*, further

supporting virus-host co-evolution theory. This study expands our understanding of virus diversity. Even though AMF is notably hard to investigate due to its biotrophic nature, this study demonstrates the utility of whole root metatranscriptome.

Keywords: Mycorrhizal fungi; mycovirus; mitovirus; *Rhizophagus*

2.1 Introduction

About eighty percent of land plants form symbiotic relationships with arbuscular mycorrhizal (AM) fungi [1], where obligate mutualistic fungi colonize plant roots for their spores to germinate and form hyphae. Examples of endophytic fungi, including AM fungi, have been shown to help control fungal pathogens [2], resist drought and salinity [3,4], and affect the overall fitness (growth, survival, etc.) of vascular plant families [5,6]. However, it is not well known whether multipartite plant-AM fungi-virus interactions may play a role in the plant's adaptation to biotic and abiotic stresses. Specifically, it remains unclear how AM fungi infections can alter patterns of plant gene expression, or whether superimposed viral infections would have cascading effects on the plant gene expression.

As AM fungi play important roles in carbon/nitrogen/phosphate cycling and compete with pathogens for ecological niches, there is emerging interest in discovering whether they harbor viruses through next generation sequencing [7,8]. It is necessary to recover the virus sequences associated with these fungi before further determining the effect of viral infections on hyphal growth and nutrient uptake of the host plant. Other endophytic fungi forming mutualistic symbiotic relationships with land plants have been shown to harbor viruses and confer heat tolerance when infected by virus(es) [9]. However, the prevalence and effects of virus infection on AM fungi are largely unknown, and the roles they play in the context of carbon/nutrient cycling are still ambiguous. Additionally, the virome of AM

fungi is difficult to study partly because of its obligate nature of biotrophic reproduction that requires a large number of hyphae [8] or spores [10].

Likely not mutually exclusive, "virus-host ancient coevolution theory" is one of two hypotheses that have been proposed for mycovirus origin [11], with the other hypothesis suggesting that plant viruses are the origin of mycoviruses [12]. The *Narnaviridae* family of mycovirus is comprised of two genera, namely *Narnavirus* and *Mitovirus*, and include some of the simplest RNA viruses ever identified [13]. Narnaviruses are known to be localized in the cytosol, expressed using standard genetic code [13] and likely evolved from a RNA bacteriophage [14]. Mitoviruses, meanwhile, are known to be found primarily in mitochondria of the fungal host, translated using mold mitochondrial genetic code, and are believed to have evolved as endosymbiont of alphaproteobacteria [13]. Additionally, *Narnaviradae* RdRps are closely related to leviviruses, viruses of bacteria and ourmiaviruses of plants [13-15].

Typical mitoviruses have < 3 kb genomes and have been detected in both fungi and plants [16], and either exist endogenously in plant genomes or freely replicate in mitochondria as genuine viruses. Endogenous mitovirus sequences may or may not be transcribed actively [17]. However, mitoviruses detected from mycorrhizal fungi generally have genome sizes greater than 3 kb, and the coding regions can be either translated by a cytosolic/nuclear genetic codon usage table or a mitochondrial table [7,18].

We recently screened soybean leaf-associated viromes and identified 23 nearly full-length mycoviral genomes using RNA-Seq of total RNA even when the plant sequences were present [19]. In order to understand the effects of a tritrophic relationship among plant-AM fungi-virus interactions on soil processes, root-associated viromes should be

profiled. Differences in phosphate and nitrogen uptake of AMF were observed even within the same species [20], suggesting that besides genetic variability, there could be microbes, including mycoviruses, hosted by AMF that affect their functions. Notably, Ikeda et al. [21] determined that AM fungi infected by the virus, GRF1V-M, produced two-fold fewer spores compared to the virus-free culture line of *Rhizophagus* spp. strain RF1, and was less efficient in promoting plant growth. Therefore, in this study, we aimed to discover and characterize new mycoviruses infecting AM fungi with combined approaches. We used a culture-independent metatranscriptomics approach to detect viruses infecting *Rhizophagus* spp., and by reanalyzing data from other *Rhizophagus* spp. available as SRR data from the NCBI database (https://www.ncbi.nlm.nih.gov/sra). As *Medicago truncatula* is a host plant for *Rhizophagus* spp., we performed metatranscriptome RNA-Seq on *M. truncatula* roots directly to screen for mycoviruses. This research could provide insight on virus evolution and may help researchers form hypotheses to study the mechanisms of the varying functions from isolates/species of AMF that affect their biofertilizer potential.

2.2. Materials and Methods

2.2.1. Plant and fungal material.

Medicago truncatula (A17) seeds were surface sterilized with concentrated H_2SO_4, rinsed with autoclaved distilled water, and kept at 4^{o}C overnight. The seeds were then pregerminated on moist filter paper for 7 days until fully grown cotyledons were developed. We transferred the seedlings into pots containing 250 mL of an autoclaved soil substrate mixture of 40% sand, 20% perlite, 20% vermiculite, and 20% soil (v:v:v:v; 4.81 mg/kg P_i after Olsen extraction, 10 mg/kg NH_4^+, 34.40 mg/kg NO_3^-, pH 8.26). At transplanting, each seedling was inoculated with 0.4 g mycorrhizal root material and ~500 spores of *Rhizophagus irregularis* N.C. Schenck & G.S. Sm. (isolate 09 collected from

Southwest Spain by Mycovitro S.L. Biotechnología ecológica, Granada, Spain). The roots and the fungal inoculum were produced in axenic Ri T-DNA transformed carrot (*Daucus carota* clone DCI) root organ cultures in Petri dishes filled with mineral medium [22]. After approximately eight weeks, the spores were isolated by blending the medium in 10 mM citrate buffer (pH 6.0).

The plants were grown in a growth chamber with a 25°C/20°C day and night cycle, 30% humidity, and a photosynthetic active radiation of 225 μmol m^{-2} s^{-1},and watered when necessary. After seven weeks, the plants were harvested and mycorrhizal root material was frozen in liquid nitrogen and stored at -80°C until RNA extraction. To quantify the mycorrhizal colonization, some roots were cleared with 10% KOH solution at 80ºC for 30 min, rinsed with water, and stained with 5% ink at 80ºC for 15 min [23]. We analyzed a minimum of 100 root segments to determine the percentage of AM root colonization by using the gridline intersection method [24].

2.2.2. High-throughput sequencing.

Approximately 150 mg of root tissue was ground in liquid nitrogen, and total RNA was extracted using the Qiagen RNeasy Plant Mini Kit (Valencia, CA, USA). RNA samples were treated with DNase I, evaluated for integrity by agarose gel electrophoresis, and rRNAs were removed by the Ribo-Zero Plant Kit (Illumina, San Diego, CA, USA), and used as templates to construct the library with a ScriptSeq RNA sample preparation kit (Illumina, San Diego, CA, USA). The library was submitted to the W. M. Keck Center, University of Illinois for quality check and cleanup and sequenced on an Illumina HiSeq 4000 for 100 bp paired-end reads.

2.2.3. Sequence analysis.

Sequence reads from the above sequencing run, as well as publicly available data (published by Tisserant et al., 2013 [25]) under SRX312982 (*Rhizophagus diaphanum* MUCL 43196; previously *Glomus diaphanum* [26]), SRX375378 (*Rhizophagus irregularis* DAOM-197198; previously *Glomus intraradices* or *Rhizophagus intraradices* [25,26]) and SRX312214 (*Rhizophagus irregularis* C2) were retrieved from the NCBI database and the paired-end sequence reads (100 nt in length) were trimmed by BBMap tools (https://sourceforge.net/projects/bbmap) and assembled into contigs using the TRINITY *de novo* transcriptome assembler [27]. Contigs with significant similarity to viral amino acid sequences were identified using USEARCH ublast option [28] with a parameter e-value of 0.0001 and compared to a custom database containing *Rhizophagus irregularis* and viral amino acid sequences from GenBank using BLASTX [29]. The nucleotide sequences of all suspected mycovirus contigs were compared with the NCBI nr database using BLASTX [29] to exclude misidentified sequences. The number of reads aligning to different target sequences was calculated using Bowtie [30]. Predicted amino acid sequences were aligned using ClustalW [31]. Aligned protein sequences were used to reconstruct a maximum likelihood tree with the model WAG + G + I + F using Mega (Molecular Evolutionary Genetics Analysis) version 7.0 software [32]. Statistical support for this analysis was computed based on 100 nonparametric bootstrap replicates. The MEME suite 5.0.1 was used to compare the motifs [33]. The viral sequences were submitted to the GenBank database under the following accession numbers: RdMV1, MH732931; RdMV2, MH732930; RdMV3, MK156099; RdMV4, MK156100; RirMV1 and MH732933.

2.2.4. Reverse-transcription PCR (RT-PCR).

To confirm that the RirMV1 sequence detected was not an artifact and indeed derived from the *Medicago* root material, RT-PCR amplified a 3.4 kb amplicon from the RNA extract after DNase treatment by the virus-specific primers, RirMV1-197F (5'-CACCTATGAGCCCGGTTAAA-3') and RirMV1-3409R (5'-GGAGAATCGTCCTTCCTTCC-3'). For the nested PCR the primers RirMV-197F and RirMV1-3228R (5'-ACCTTTCCAGGGGAGACCTA-3') were used. The nested amplicon was submitted for Sanger sequencing to confirm the identity after ExoSap-IT cleanup (Thermofisher, Waltham, MA, USA). Additionally, to confirm that the viral sequence is not from the *Medicago* host, reverse transcription of cDNA was made by using Maxima H Minus Reverse Transcriptase (Thermo Scientific, Waltham, MA, USA) at 50 ^{o}C for 30 min followed by 85 ^{o}C for 5 min inactivation. Then PCR was performed using RirMV1-197F and RirMV1-3228R primer set and Phire Plant Direct PCR Kit (Thermo Scientific, Waltham, MA, USA).

2.2.5 Rapid amplification of cDNA ends (RACE).

To complete the genome sequence of RirMV1, the 5'- and 3'- terminal sequences were determined using the FirstChoice RLM-RACE (rapid amplification of cDNA ends) kit (Life Technologies). Primers 336R (5'-AGAGCGGTCGCTTCTGTCTA-3') and 216R (5'-TTTAACCGGGCTCATAGGTG-3') were used for 5'-RACE as outer and inner primers, respectively. Primers 3210F (5'-TAGGTCTCCCCTGGAAAGGT-3') and 3347F (5'-CGACCTCTGGAGGTTGAAAG-3') were used for 3'-RACE as outer and inner primers, respectively.

2.3. Results

2.3.1. Mycoviruses in the metatranscriptome of *Rhizophagus irregularis* inoculated roots

After colonization of *R. irregularis* was confirmed by microscopy (Figure S1), sequencing of the mycorrhizal *Medicago truncatula* roots on the Illumina HiSeq4000 platform resulted in a total of 85 million paired-end reads, yielding 12.1 GB of sequence information. The data were submitted to the SRA database at NCBI (accession number: SRX4679168). In this data set, we identified one viral contig (RirMV1). To confirm the viral contig assembled from the short reads, RirMV1-3409R primed cDNA was used as a PCR template to amplify most of the viral contig. The primers RirMV1-197F and RirMV1-3409R amplified multiple bands, and among them there was a faint 3 kb band (not shown). The 3 kb band was subsequently excised, and the gel was purified. Nested PCR using RirMV1-197F and RirMV1-3228R resulted in a clear band of 3 kb (Figure 1A). Sanger sequencing using the same primer set confirmed the band as RirMV1 cDNA amplicon. PCR attempts to amplify RirMV1 directly from the DNA of the *R. irregularis* strain 09 infected *Medicago* roots were not successful, indicating that the viral transcript was not derived from virus segments integrated into the host genome that are actively expressed. Instead they are from the genuine virus (Figure 1B). We also attempted to amplify a smaller target using viral-specific primers 197F and 336R for 140 bp amplicon and ran a 1.5% gel to confirm that there was no amplification, leading to the same conclusion that the viral sequence was not from *Medicago*, which confirms that *R. irregularis* is the host of the virus. Additionally, we also attempted RACE amplification of RirMV1 contig, but failed to extend the contig.

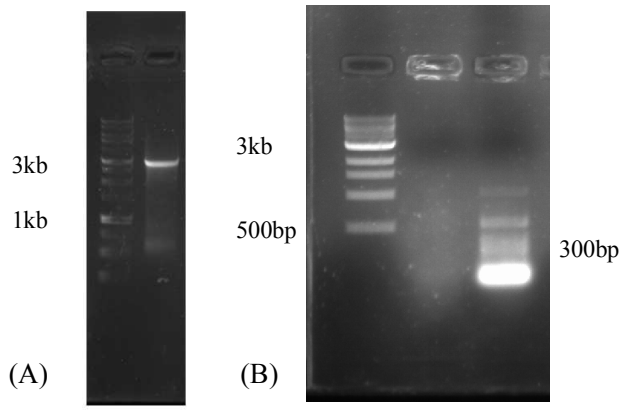

Figure 1. (A) Agarose gel electrophoresis of the RT-PCR product showing a ~3 kb nested PCR amplicon that was confirmed by Sanger sequencing as cDNA amplicon of RirMV1. Left lane: 1 kb ladder. Right Lane: RirMV1 amplicon of the predicted size of 3 kb and (B) Agarose gel electrophoresis of the RT-PCR product showing no amplification, suggesting the viral contig of RNA-Seq was not originated from *Medicago* root without *R. irregularis* strain 09 infection. Left to right lanes: 1 kb Ladder, viral primers, plant primers.

2.3.2. Mycoviruses in the transcriptomes of *Rhizophagus* spp.

To identify mycoviruses in *Rhizophagus* spp., we first reanalyzed the publicly available RNA-Seq data sets of *R. irregularis* strain-C2 (SRX312214), *R. irregularis* DAOM-197198 (SRX375378) and *R. diaphanum* MUCL 43196 (SRX312982). No viruses could be identified in the available *Rhizophagus irregularis* DAOM-197198 transcriptome, but we found multiple novel mycoviruses in the transcriptome of *R. diaphanum* MUCL 43196 (Rhizophagus diaphanum mitovirus 1 - RdMV1, 3,554 nt long; Rhizophagus diaphanum mitovirus 2 - RdMV2, 4,382 nt long; Rhizophagus diaphanum mitovirus 3 – RdMV3, 3,652 nt long and Rhizophagus diaphanum mitovirus 4 – RdMV4, 3,443 nt long) that had similarity to members of the *Mitovirus* genus (Table 1).

Overall, RirMV1 had 41,322 reads and a 0.10% alignment with the sequencing run of the colonized Medicago roots. Among the total reads for SRX312982 from *R. diaphanum*, 1,475 read-counts aligned to RdMV1 (0.0015%), 3,649 to RdMV2 (0.0036%), 2350 to

RdMV3 (0.0023%), and 462 to RdMV4 (0.00045%), see Table 1. The NCBI BLAST results indicate that these contigs are putatively similar in function to previously identified RNA-dependent RNA polymerase of mitoviruses.

Table 1. Identified mycovirus-like sequences, contig lengths, and their putative functions are shown in the table below, including the data source from which the virus sequence was recovered. These new contigs were identified as mitoviruses (MV) and were recovered from two different fungal hosts (Rd, *Rhizophagus diaphanum*; Rir, *Rhizophagus irregularis*).

Contig name	Data source	Contig length (nt)	Read counts	NCBI accession	Amino acid Identity (%)	Putative function (most similar virus)
RdMV1	SRX312982 (*Rhizophagus diaphanum* MUCL 43196)	3554	1,475	MH732931	32	RNA-dependent RNA polymerase [Rhizoctonia solani mitovirus 12]
RdMV2	SRX312982 (*Rhizophagus diaphanum* MUCL 43196	4382	3,649	MH732930	28	RNA-dependent RNA polymerase [Gigaspora margarita mitovirus 2]
RdMV3	SRX312982 (*Rhizophagus diaphanum* MUCL 43196	3652	2350	MK156099	36	RNA-directed RNA polymerase [Rhizophagus sp. RF1 mitovirus]
RdMV4	SRX312982 (*Rhizophagus diaphanum* MUCL 43196	3443	462	MK156100	30	RNA-dependent RNA polymerase [Rhizoctonia mitovirus 1]
RirMV1	Sequenced transcriptome (submitted under accession: SRX4679168)	3685	41,322	MH732933	31	RNA-dependent RNA polymerase [Rhizoctonia solani mitovirus 12]

2.3.3. Phylogenetic analysis and the characterization of conserved RdRp region of mitoviruses

To identify the evolutionary lineages among the identified mitoviruses, we analyzed the protein sequences of mitoviruses to reconstruct the phylogenetic tree (Figure 2). While there was no virus found in SRX375378 and SRX312214, there were four partial genome sequences identified from SRX312982 publicly available data similar to viruses from the family *Narnaviridae*. Two of these sequences (RdMV1 and RdMV2) formed a separate clade with RirMV1 and previously identified mitoviruses from *Gigaspora margarita* (GmMV2, GmMV3, and GmMV4). The other two contigs (RdMV3 and RdMV4) were phylogenetically similar to the mitovirus infecting *Rhizophagus clarus* (RcMV1) (Figure 2). We also compared the genome structure of identified mitoviruses to see if the RdRp region is uniformly conserved (Figure 3). To confirm the presence of functionally conserved motifs of RNA-dependent RNA polymerase (RdRp) in identified viruses, we further analyzed and compared six RdRp motifs (A–F) with other mitoviruses of pathogenic fungi in the NCBI database (Figure 4). Three of these motifs (A–C) are among the most conserved motifs of RdRp and include residues involved in catalytic activation and dNTP/rNTP recognition (discussed in detail below) by RdRp [34,35]. Noticeable differences in the amino acid sequence include a histidine in the mitoviruses of *Rhizophagus* spp. instead of a serine at residue 325 and a glutamic acid instead of an aspartic acid at residue 329 within the RdRp motif F.

The RdRps can be translated using either a cytosolic or mitochondrial code. The complete coding RdRp was 811 aa long for RirMV1, compared to the average of ~700 aa for the most closely related mitoviruses infecting *Sclerotinia sclerotiorum*. RdMV1 and RirMV1 have nearly identical lengths of RdRp, these being 812 aa and 811 aa, respectively.

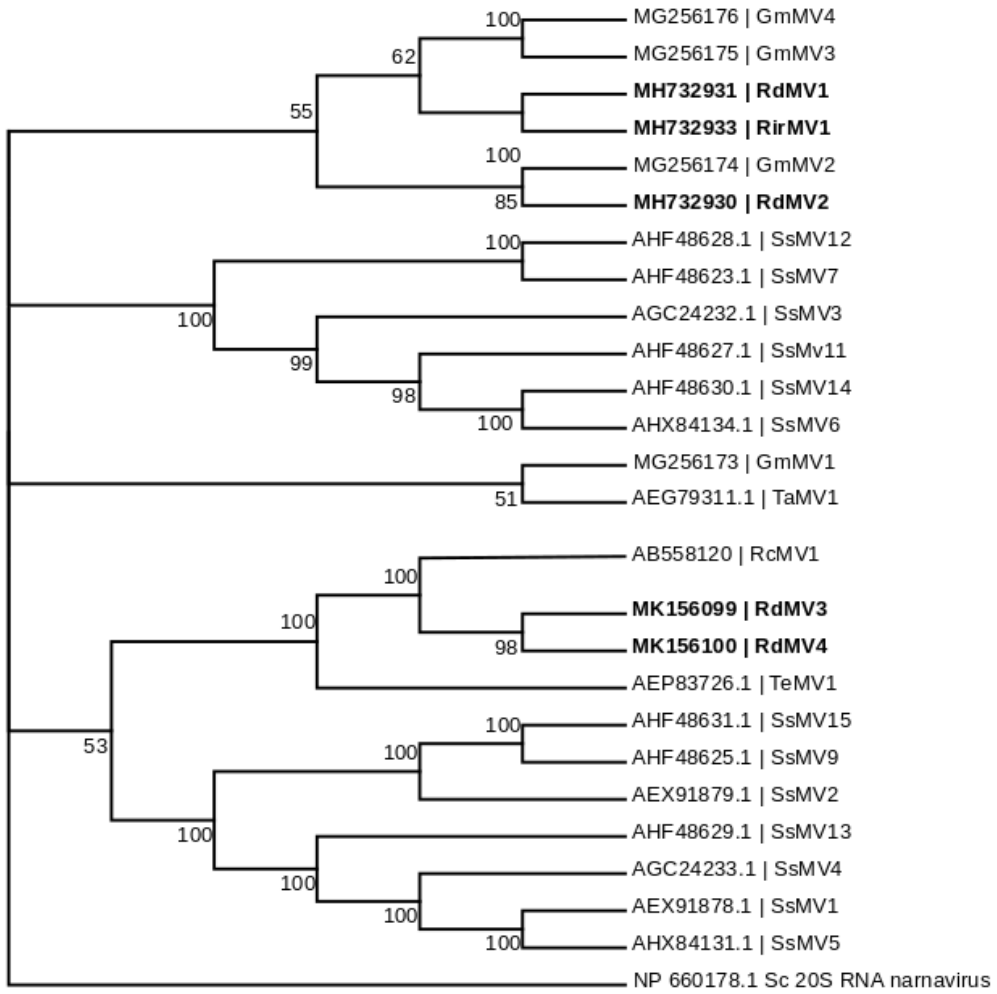

Figure 2 Maximum likelihood tree (with bootstrap consensus) depicting the relationships of the predicted amino acid sequences of RNA-dependent RNA polymerase (RdRp) of the *Rhizophagus* mitoviruses, and other confirmed and proposed members of the *Narnaviridae*. Predicted RdRp amino acid sequences were aligned with ClustalW [31], and the phylogenetic tree was inferred using Mega 7.0 software [32]. Branch lengths are scaled to the expected underlying number of amino acid substitutions per site. The Saccharomyces 20S RNA narnavirus RdRp amino acid sequence was used as an outgroup to root the tree. Five newly identified mitoviruses (in bold) formed two separate monophyletic clusters between the Rhizophagus-associated mitoviruses. The following abbreviations were used for the Mitovirus (MV) sequences: Sc, *Saccharomyces cerevisiae*; Gm, *Gigaspora margarita*; Rd, *Rhizophagus diaphanum*; Rc, *Rhizophagus clarus*; Sc, *Sclerotinia sclerotiorum*; Rir, *Rhizophagus irregularis;* Ta, *Tuber aestivum*; Te, *Tuber excavatum*.

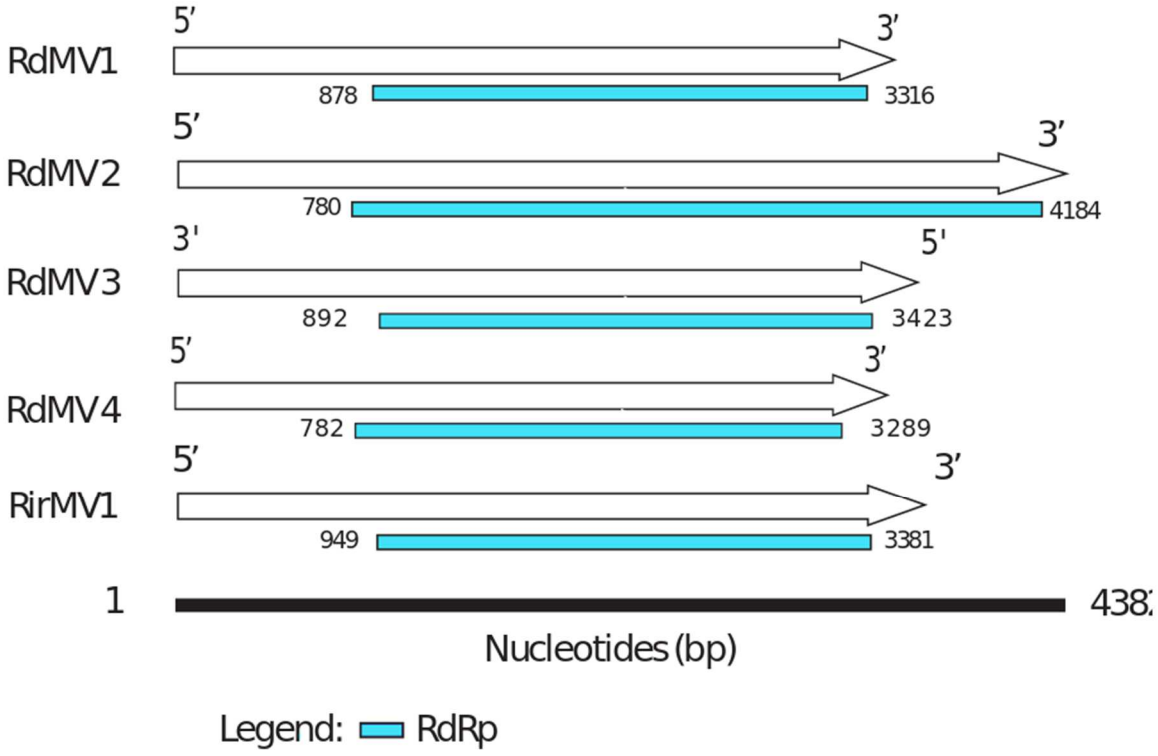

Figure 3 The genome organization of *Rhizophagus* spp. mitoviruses. The comparisons are of the organizations of RdMV1, RdMV2, RdMV3, RdMV4 and RirMV1. RdRp coding regions are labeled in blue (see also Table 1).

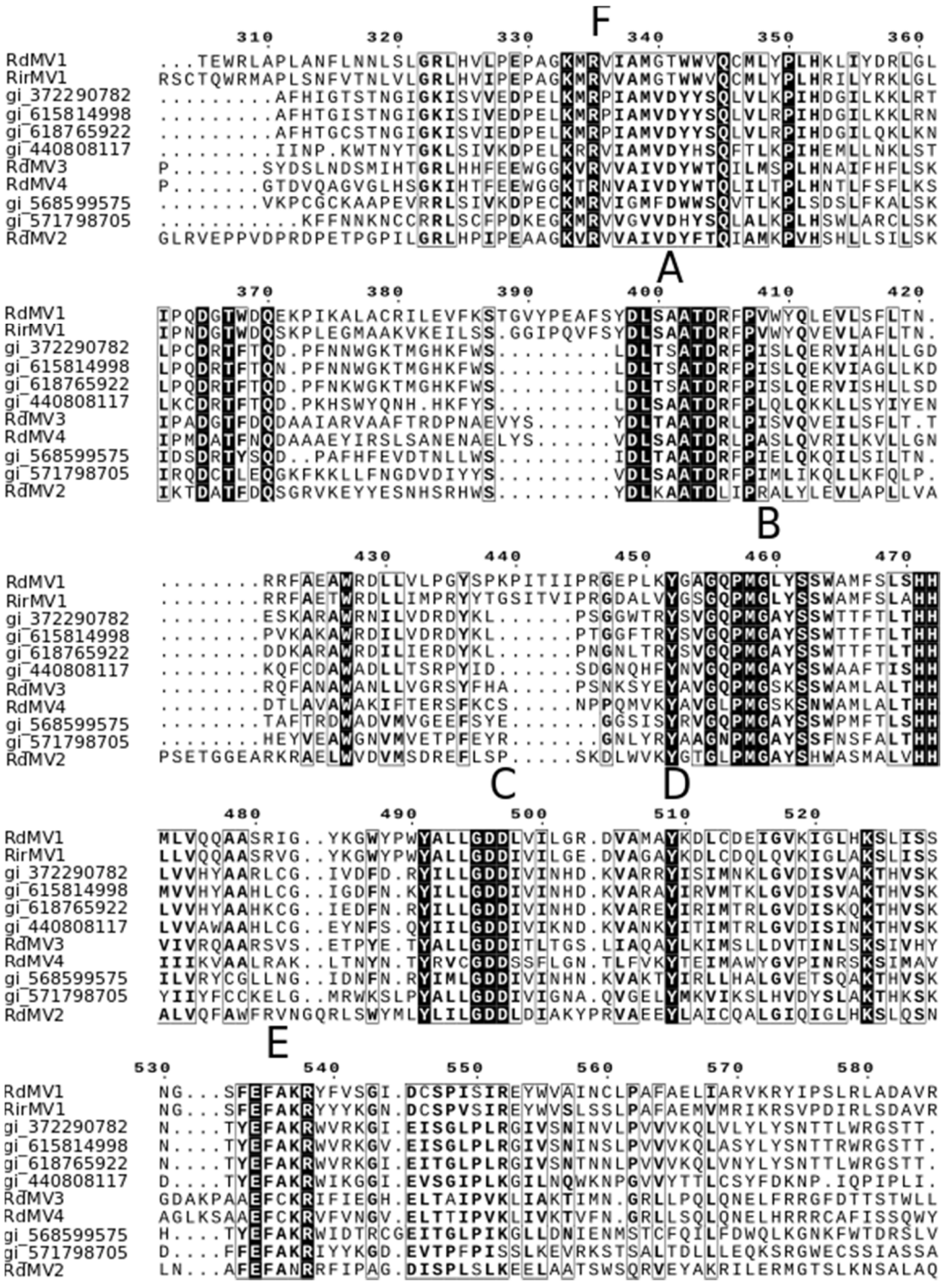

Figure 4 Conserved motifs identified in the RdRp domain of the genus *Mitovirus* based on the multiple sequence alignment of the amino acid sequences. Similar to the other mitoviruses, six conserved motifs were found. These conserved regions were labeled A-F as RdRp associated motifs described previously [36].

2.4. Discussion

Our own studies revealed a high intraspecific diversity in the growth and nutrient uptake benefits after colonization with different AM isolates [37]. As we report the identification of mycoviruses in a lab culture and *in silico* from *Rhizophagus* spp., it would be interesting to determine whether mitoviruses play any role in the variability of these responses. In this study, we identified a novel mitovirus from the sequenced transcriptome of *R. irregularis* and confirmed the presence of RT-PCR amplicon of 3kb with gel electrophoresis (Figure 1A). Additionally, Agarose gel electrophoresis of the RT-PCR product from the non-mycorrhizal *Medicago* root without *Rhizophagus* infection showed no amplification of viral contig, suggesting the newly identified viral contig (RirMV1) was not from the plant, but from *R. irregularis* (Figure 1B). We also identified four novel mitoviruses: RdMV1, RdMV2, RdMV3 and RdMV4 from *R. diaphanum* from the publicly available SRA database in NCBI (Table 1).

After the viral contigs were assembled, RT-PCR was used to verify the presence of any putative viral sequence. Also, it is necessary to rule out the possibility that the putative mycovirus genomes identified in this study could have been derived from mycoviruses integrated into the AMF genome. Oligonucleotide primers specific to the putative viral sequences need to be used to amplify the sequences using fungal genomic DNA as the template. The infection of these viruses could have resulted in beneficial/neutral effects on the host as they were selected to be sequenced without regards to apparent abnormal growth. These novel viral sequences may be used to establish Koch's postulates in future studies and to provide bases for mechanisms responsible in different nutrient uptake and plant biomass responses.

Using a mitochondrial translation table, the amino acid sequences of the three of five predicted mitovirus-like contigs clustered with mitoviruses of filamentous fungi, and constituted two distinct subclades along with mitoviruses infecting *G. margarita* (Figure 2). Our analysis showed that RdMV3 and RdMV4 are closely related to Rhizophagus clarus mitovirus 1-RF1 (RcMV1; AB558120) which is closely related to another mitovirus that was found in the ectomycorrhizal fungus *Tuber excavatum* (TeMV1; AEP83726.1). Their corresponding fungal hosts are all AM fungi and these mitoviruses all have distinctly longer RdRps than other mitoviruses that use mitochondrial translation code only. Similar to what was reported by Ikeda et al. [21], we found that the largest ORF of the two mitoviruses can also be predicted by applying the universal genetic code. Generally, functional translation of RdRp in mitoviruses involves activation of a mitochondrial genetic code [38], and as a result, tryptophan residues in mitoviruses (such as TeMV, CpMV, and HmMV1-18) are coded either by a UGA (which in universal genetic code means termination) or a UGG codon [7]. Recently identified mitoviruses from AMF, including RcMV1-RF1 [7] and the mitoviruses identified in *G. margarita* [10], all use the UGG codon for tryptophan which is compatible with both cytoplasmic and mitochondrial translation. All five novel mitoviruses identified from our study were found to use UGG for tryptophan. Interestingly, Nibert (2017) provided sequence-based explanation of this subgroup of mitoviruses using UGG instead of UGA for tryptophan in mitochondria, which is likely due to the mitochondrial codon of UGA for tryptophan in the respective fungal hosts that is correspondingly rare. Therefore, Nibert (2017) speculated that this unique group of mitoviruses do not actually replicate in cytosol [39].

Our results support the virus-host coevolution theory for the origin of these mitoviruses infecting nonpathogenic AMF fungi because the viruses they harbor do not cluster with mitoviruses from pathogenic fungi. First, amino acid sizes for the RdRps are very similar between the three viruses, RirMV1, RdMV1 and RdMV3, and the RdRp motifs are highly conserved between them (Figure 3). Besides the conserved motifs I to IV identified in Kitahara et al. [7] and Gorbalenya et al. [34], we also identified the motifs D and E (Figure 4) as shown in Bartholomaus et al. (2016) [36]. Out of these six motifs, A, B and C are among the most conserved structural motifs of the palm subdomain of RdRp with active catalytic sites [34]. Motif A (DX_5D) contains two aspartic acid residues separated by any five amino acids, while motif C contains two aspartic acid residues, consecutively. These residues are known to form divalent bonds between Mg2+ ions and/or Mn2+ ions for catalytic activation of the domain [34]. Similarly, motif B is known to form a long and conserved alpha-helix sequence with an asparagine residue which is indispensable for discriminating dNTPs and rNTPs that determine whether DNA or RNA is produced [35]. Although these motifs are known to be required for polymerase activity, the other three motifs (D, E and F) are not well studied in terms of their function.

Experiments to assess the impacts of viral infection on fungal colonization and sporulation and on the ability of virus-infected fungal isolates to affect nutrient cycling in host crops can be done by using virus-induced gene silencing (VIGS) approaches to knockdown the expression of viral transcripts. VIGS systems have been successfully applied in *R*. *clarus* to study fungal gene functions [40], which could be modified to instead silence RirMV1 using *Nicotiana benthamiana* as the plant host to deliver the silencing construct through the Cucumber mosaic virus Y strain based VIGS system [41]. The

silencing effect will be effective if RirMV1 replicates in the cytoplasm as well, but will be ineffective if it replicates only in mitochondria since the RNA silencing machinery is not present in mitochondria and the double-layered membrane is a barrier. This may also resolve the long-standing question of whether mitoviruses in AMF replicate in the cytoplasm, which can shed light on the evolution of capsidless positive-strand RNA viruses.

Supplementary Materials

The following are available online at https://www.mdpi.com/1999-4915/10/12/707/s1, Figure S1: Stain of cross-section of the roots to confirm the AM fungal infection showing the (A) density of arbuscules as the small oval-shaped objects and (B) close-up view of hyphae and connected arbuscules.

Author Contributions

A.N. and S.-Y.L.M. conceived and designed the experiments; A.N., C.F., A.K. and J.F. performed the experiments; A.N. and S.-Y.L.M. analyzed the RNA-Seq data; H.B., A.N. and S.-Y.L.M. wrote the paper.

Funding

This study was supported in part by National Sclerotinia Initiative Grant SA1800330 (to Shin-Yi Lee Marzano) and SDSU startup from USDA Hatch fundSD00H606-16 project number with Accession Number 1009451 (to Shin-Yi Lee Marzano). The authors also acknowledge support from the South Dakota Research and Promotion Council (to H.B.) for these studies.

Conflicts of Interest: The authors declare no conflict of interest.

References

1. Smith, S.; Read, D. Mycorrhizal symbiosis (academic, san diego). *SmithMycorrhizal Symbiosis1997* **1997**.
2. Azcón-Aguilar, C.; Barea, J. Arbuscular mycorrhizas and biological control of soil-borne plant pathogens–an overview of the mechanisms involved. *Mycorrhiza* **1997**, *6*, 457-464.
3. Augé, R.M. Water relations, drought and vesicular-arbuscular mycorrhizal symbiosis. *Mycorrhiza* **2001**, *11*, 3-42.
4. Porcel, R.; Aroca, R.; Ruiz-Lozano, J.M. Salinity stress alleviation using arbuscular mycorrhizal fungi. A review. *Agronomy for Sustainable Development* **2012**, *32*, 181-200.
5. SCHÜßLER, A.; SCHWARZOTT, D.; WALKER, C. A new fungal phylum, the glomeromycota: Phylogeny and evolution. *Mycological Research* **2001**, *105*, 1413-1421.
6. Hildebrandt, U.; Kaldorf, M.; Bothe, H. The zinc violet and its colonization by arbuscular mycorrhizal fungi. *Journal of Plant Physiology* **1999**, *154*, 709-717.
7. Kitahara, R.; Ikeda, Y.; Shimura, H.; Masuta, C.; Ezawa, T. A unique mitovirus from glomeromycota, the phylum of arbuscular mycorrhizal fungi. *Arch Virol* **2014**, *159*, 2157-2160.
8. Ezawa, T.; Ikeda, Y.; Shimura, H.; Masuta, C. Detection and characterization of mycoviruses in arbuscular mycorrhizal fungi by deep-sequencing. *Plant Virology Protocols: New Approaches to Detect Viruses and Host Responses* **2015**, 171-180.
9. Márquez, L.M.; Redman, R.S.; Rodriguez, R.J.; Roossinck, M.J. A virus in a fungus in a plant: Three-way symbiosis required for thermal tolerance. *science* **2007**, *315*, 513-515.
10. Turina, M.; Ghignone, S.; Astolfi, N.; Silvestri, A.; Bonfante, P.; Lanfranco, L. The virome of the arbuscular mycorrhizal fungus gigaspora margarita reveals the first report of DNA fragments corresponding to replicating non□retroviral rna viruses in fungi. *Environmental microbiology* **2018**.
11. Pearson, M.N.; Beever, R.E.; Boine, B.; Arthur, K. Mycoviruses of filamentous fungi and their relevance to plant pathology. *Molecular Plant Pathology* **2009**, *10*, 115-128.
12. Roossinck, M.J. Evolutionary and ecological links between plant and fungal viruses. *New Phytologist* **2018**.
13. Hrabakova, L.; Koloniuk, I.; Petrzik, K. Phomopsis longicolla rna virus 1 - novel virus at the edge of myco- and plant viruses. *Virology* **2017**, *506*, 14-18.
14. Koonin, E.V.; Dolja, V.V.; Krupovic, M. Origins and evolution of viruses of eukaryotes: The ultimate modularity. *Virology* **2015**, *479-480*, 2-25.
15. Rastgou, M.; Habibi, M.K.; Izadpanah, K.; Masenga, V.; Milne, R.G.; Wolf, Y.I.; Koonin, E.V.; Turina, M. Molecular characterization of the plant virus genus ourmiavirus and evidence of inter-kingdom reassortment of viral genome segments as its possible route of origin. *Journal of General Virology* **2009**, *90*, 2525-2535.

16. Nibert, M.L.; Vong, M.; Fugate, K.K.; Debat, H.J. Evidence for contemporary plant mitoviruses. *Virology* **2018**, *518*, 14-24.
17. Bruenn, J.A.; Warner, B.E.; Yerramsetty, P. Widespread mitovirus sequences in plant genomes. *PeerJ* **2015**, *3*, e876.
18. Lakshman, D.K.; Jian, J.H.; Tavantzis, S.M. A double-stranded rna element from a hypovirulent strain of rhizoctonia solani occurs in DNA form and is genetically related to the pentafunctional arom protein of the shikimate pathway. *Proc. Natl. Acad. Sci. U. S. A.* **1998**, *95*, 6425-6429.
19. Marzano, S.-Y.L.; Domier, L.L. Reprint of "novel mycoviruses discovered from metatranscriptomics survey of soybean phyllosphere phytobiomes". *Virus research* **2016**, *219*, 11-21.
20. Mensah, J.A.; Koch, A.M.; Antunes, P.M.; Kiers, E.T.; Hart, M.; Bucking, H. High functional diversity within species of arbuscular mycorrhizal fungi is associated with differences in phosphate and nitrogen uptake and fungal phosphate metabolism. *Mycorrhiza* **2015**, *25*, 533-546.
21. Ikeda, Y.; Shimura, H.; Kitahara, R.; Masuta, C.; Ezawa, T. A novel virus-like double-stranded rna in an obligate biotroph arbuscular mycorrhizal fungus: A hidden player in mycorrhizal symbiosis. *Molecular plant-microbe interactions* **2012**, *25*, 1005-1012.
22. St-Arnaud, M.; Hamel, C.; Vimard, B.; Caron, M.; Fortin, J. Enhanced hyphal growth and spore production of the arbuscular mycorrhizal fungus glomus intraradices in an in vitro system in the absence of host roots. *Mycological research* **1996**, *100*, 328-332.
23. Vierheilig, H.; Coughlan, A.P.; Wyss, U.; Piché, Y. Ink and vinegar, a simple staining technique for arbuscular-mycorrhizal fungi. *Applied and environmental microbiology* **1998**, *64*, 5004-5007.
24. McGonigle, T.P.; Miller, M.H.; Evans, D.G.; Fairchild, G.L.; Swan, J.A. A new method which gives an objective measure of colonization of roots by vesicular-arbuscular mycorrhizal fungi. 1990, p 495.
25. Tisserant, E.; Malbreil, M.; Kuo, A.; Kohler, A.; Symeonidi, A.; Balestrini, R.; Charron, P.; Duensing, N.; Frey, N.F.D.; Gianinazzi-Pearson, V.*, et al.* Genome of an arbuscular mycorrhizal fungus provides insight into the oldest plant symbiosis. *Proc. Natl. Acad. Sci. U. S. A.* **2013**, *110*, 20117-20122.
26. Schüßler, A.; Walker, C. In *The glomeromycota: A species list with new families and new genera*, Libraries at The Royal Botanic Garden Edinburgh, The Royal Botanic Garden Kew, Botanische Staatssammlung Munich, and Oregon State University: Kew, UK, 2010; pp 1-56.
27. Grabherr, M.G.; Haas, B.J.; Yassour, M.; Levin, J.Z.; Thompson, D.A.; Amit, I.; Adiconis, X.; Fan, L.; Raychowdhury, R.; Zeng, Q.*, et al.* Full-length transcriptome assembly from rna-seq data without a reference genome. *Nat Biotechnol* **2011**, *29*, 644-652.
28. Edgar, R.C. Search and clustering orders of magnitude faster than blast. *Bioinformatics* **2010**, *26*, 2460-2461.
29. Altschul, S.F.; Gish, W.; Miller, W.; Myers, E.W.; Lipman, D.J. Basic local alignment search tool. *J. Mol. Biol.* **1990**, *215*, 403-410.

30. Langmead, B.; Trapnell, C.; Pop, M.; Salzberg, S.L. Ultrafast and memory-efficient alignment of short DNA sequences to the human genome. *Genome Biology* **2009**, *10*, R25.
31. Larkin, M.A.; Blackshields, G.; Brown, N.P.; Chenna, R.; McGettigan, P.A.; McWilliam, H.; Valentin, F.; Wallace, I.M.; Wilm, A.; Lopez, R.*, et al.* Clustal w and clustal x version 2.0. *Bioinformatics* **2007**, *23*, 2947-2948.
32. Kumar, S.; Stecher, G.; Tamura, K. Mega7: Molecular evolutionary genetics analysis version 7.0 for bigger datasets. *Mol Biol Evol* **2016**, *33*, 1870-1874.
33. Bailey, T.L.; Boden, M.; Buske, F.A.; Frith, M.; Grant, C.E.; Clementi, L.; Ren, J.; Li, W.W.; Noble, W.S. Meme suite: Tools for motif discovery and searching. *Nucleic acids research* **2009**, *37*, W202-W208.
34. Gorbalenya, A.E.; Pringle, F.M.; Zeddam, J.L.; Luke, B.T.; Cameron, C.E.; Kalmakoff, J.; Hanzlik, T.N.; Gordon, K.H.J.; Ward, V.K. The palm subdomain-based active site is internally permuted in viral rna-dependent rna polymerases of an ancient lineage. *Journal of Molecular Biology* **2002**, *324*, 47-62.
35. Gohara, D.W.; Crotty, S.; Arnold, J.J.; Yoder, J.D.; Andino, R.; Cameron, C.E. Poliovirus rna-dependent rna polymerase (3dpol): Structural, biochemical, and biological analysis of conserved structural motifs a and b. *J Biol Chem* **2000**, *275*, 25523-25532.
36. Bartholomaus, A.; Wibberg, D.; Winkler, A.; Puhler, A.; Schluter, A.; Varrelmann, M. Deep sequencing analysis reveals the mycoviral diversity of the virome of an avirulent isolate of rhizoctonia solani ag-2-2 iv. *PLoS One* **2016**, *11*, e0165965.
37. Fellbaum, C.R.; Mensah, J.A.; Cloos, A.J.; Strahan, G.E.; Pfeffer, P.E.; Kiers, E.T.; Bücking, H. Fungal nutrient allocation in common mycorrhizal networks is regulated by the carbon source strength of individual host plants. *New Phytologist* **2014**, *203*, 646-656.
38. Shackelton, L.A.; Holmes, E.C. The role of alternative genetic codes in viral evolution and emergence. *Journal of Theoretical Biology* **2008**, *254*, 128-134.
39. Nibert, M.L. Mitovirus uga (trp) codon usage parallels that of host mitochondria. *Virology* **2017**, *507*, 96-100.
40. Kikuchi, Y.; Hijikata, N.; Ohtomo, R.; Handa, Y.; Kawaguchi, M.; Saito, K.; Masuta, C.; Ezawa, T. Aquaporin□mediated long□distance polyphosphate translocation directed towards the host in arbuscular mycorrhizal symbiosis: Application of virus□induced gene silencing. *New Phytologist* **2016**, *211*, 1202-1208.
41. Otagaki, S.; Arai, M.; Takahashi, A.; Goto, K.; Hong, J.-S.; Masuta, C.; Kanazawa, A. Rapid induction of transcriptional and post-transcriptional gene silencing using a novel cucumber mosaic virus vector. *Plant biotechnology* **2006**, *23*, 259-265.

CHAPTER THREE: ROLES OF ARGONAUTES AND DICERS ON *SCLEROTINIA SCLEROTIORUM* ANTIVIRAL RNA SILENCING

This chapter has been published in the journal *Frontiers in Plant Science*:

Neupane, A., Feng, C., Mochama, P.K., Saleem, H., and Lee Marzano, S.Y. (2019). Roles of Argonautes and Dicers on *Sclerotinia sclerotiorum* Antiviral RNA Silencing. *Front Plant Sci* 10, 976.

Abstract

RNA silencing or RNA interference (RNAi) is an essential mechanism in animals, fungi, and plants that functions in gene regulation and defense against foreign nucleic acids. In fungi, RNA silencing has been shown to function primarily in defense against invasive nucleic acids. We previously determined that mycoviruses are triggers and targets of RNA silencing in *Sclerotinia sclerotiorum*. However, recent progresses in RNAi or dsRNA-based pest control requires more detailed characterization of the RNA silencing pathways in *S. sclerotiorum* to investigate the utility of dsRNA-based strategy for white mold control. This study elucidates the roles of argonaute enzymes, *agl*-2 and *agl*-4, in small RNA metabolism in *S. sclerotiorum*. Gene disruption mutants of *agl*-2 and *agl*-4 were compared for changes in phenotype, virulence, viral susceptibility, and small RNA profiles. The Δ*agl*-2 mutant but not the Δ*agl*-4 mutant had significantly slower growth and virulence prior to virus infection. Similarly, the Δ*agl*-2 mutant but not the Δ*agl*-4 mutant, showed greater debilitation under virus infection compared to uninfected strains. The responses were confirmed in complementation studies and revealed the antiviral role of *agl*-2. Gene disruption mutants of *agl*-2, *agl*-4, Dicer-like (*dcl*)-1 and *dcl*-2 did not change the stability of the most abundant endogenous small RNAs, which suggests the existence of alternative enzymes/pathways for small RNA biogenesis in *S.*

sclerotiorum. Furthermore, *in vitro* synthesized dsRNA targeting *agl*-2 showed a significantly reduced average lesion diameter ($P<0.05$) on canola leaves with *agl*-2 down-regulated compared to controls. This is the first report describing the effectiveness of RNA pesticides targeting *S. sclerotiorum* RNA silencing pathway for the control of the economically important pathogen.

Keywords: RNA pesticide, Argonautes, dicers, mycovirus, *Sclerotinia sclerotiorum*, RNA silencing, tRNA halves

3.1 Introduction

RNA silencing is a transcriptional and post-transcriptional suppression of gene expression. One of the roles that RNA silencing plays has long been identified as an adaptive defense mechanism against foreign nucleic acids, including viruses in animals, fungi, and plants (Waterhouse et al., 2001;Baulcombe, 2004;2005). Unlike in animals and plants, the evolved RNA silencing in fungi to date has demonstrated that it is almost dispensable for endogenous gene regulation because gene disruption mutants often grow just fine. Instead, only when the mutants of RNA silencing genes are under virus infection, the antiviral role of those genes play then become evident (Segers et al., 2007;Zhang et al., 2014;Yu et al., 2018). However, studies of *Neurospora crassa* and other filamentous fungi have revealed diverse small RNA biogenesis pathways, suggesting that fungi adapt RNAi silencing pathways for several cellular processes with some of the RNA silencing genes playing dual roles (reviewed in (Dang et al., 2011)). On the other hand, fungal RNA silencing genes can also have redundant functions, such as antiviral, processing of dsRNA or transgenes (Catalanotto et al., 2004;Wang et al., 2016;Yu et al., 2018).

Sclerotinia sclerotiorum is a devastating plant fungal pathogen that causes up to 100% yield losses in crop production affecting a wide array of crops (Heffer Link and Johnson, 2007). Recent studies demonstrated that cross-kingdom RNA silencing can be blocked to control *Botrytis cinerea* which is a closely related to *S. sclerotiorum* (Amselem et al., 2011). The virulence of *B. cinerea* can be greatly suppressed by silencing both *B. cinerea* Dicers at the same time (Wang et al., 2016). A similar observation was made in *S. sclerotiorum* following simultaneous disruption of both its Dicers to result in reduced pathogenicity (Mochama et al., 2018). Therefore, RNA silencing pathway has great potential to be manipulated to control fungal pathogens. As *Sclerotinia sclerotiorum* has two predicted Argonautes (GenBank accession numbers Ss1G_00334 and Ss1G_11723), it is intriguing whether corresponding argonaute genes affect *S. sclerotiorum* virulence and whether it could add to the tool box of disease control with other novel strategies.

The Argonaute protein family constitutes four domains, N-terminal domain, Mid domain, and RNA-binding domains known as PAZ domains, and slicer domains known as PIWI domains (Poulsen et al., 2013). Argonaute proteins stabilize small dsRNA molecules produced by Dicer proteins to form RNA-induced silencing complexes (RISC) which are involved in post-transcriptional gene silencing or RNA-induced transcriptional silencing complexes involved in transcriptional gene silencing including chromatin modification in animals, plants, and insects (Irvine et al., 2006). When small dsRNA molecules produced by Dicers are incorporated into these effector complexes, one strand of the RNA molecule is removed and the remaining strand guides the complex to

complementary RNA sequences which are subsequently cleaved by the Argonaute RNase H-like activity (Qihong et al., 2009).

Argonaute homologs have been identified in various fungi and they differ in function and number. The basal fungus, *Mucor circinelloides*, has three argonaute genes while *Cryphonectria parasitica* has four argonaute genes and *Colletotrichum higginsianum* has two (Qihong et al., 2009;Trieu et al., 2015;Campo et al., 2016b). QDE-2 is a fungal argonaute homolog in *N. crassa* involved in quelling- the silencing of repetitive sequences such as transgenes (Fulci and Macino, 2007). In *N. crassa*, a separate silencing pathway called meiotic silencing of unpaired DNA (MSUD) has been characterized, and *N. crassa* RNA silencing components not involved in quelling have been shown to be involved in this pathway (Fulci and Macino, 2007). Similarly, in other fungi, not all components of the RNA silencing machinery are involved in RNA silencing mediated viral defense mechanisms. In *Fusarium graminearum*, only one of two argonaute genes, FgAgo1, is important in RNA silencing of viral nucleic acids (Yu et al., 2018) while in *C. parasitica* only *agl*-2 is required for antiviral RNA silencing, and in *C. higginsianum*, *agl*-1 but not *agl*-2 is essential for antiviral RNA silencing (Qihong et al., 2009;Trieu et al., 2015;Campo et al., 2016a;Campo et al., 2016b). The primary functions of the other gene homologs have not been fully characterized. As *S. sclerotiorum* are predicted to have two argonaute genes, *agl*-2 and *agl*-4, it presents a potential strategy to impede the proper small RNA processing after characterizing the roles of argonautes in *S. sclerotiorum*.

The goals of this study were to determine the function of argonaute genes in endogenous small RNA processing and defending virus infection in *S. sclerotiorum*, and

as a proof of concept, to demonstrate a control strategy from silencing a specific argonaute gene. To achieve them, we made gene displacement mutants of argonaute genes in this study and transfected *S. sclerotiorum* with a RNA virus (SsHV2-L) and compared the changes in morphology and pathogenicity. Gene displacement mutants revealed that only *agl*-2 is important in vegetative growth, as well as antiviral defense, whereas the biological function of *agl*-4 remains unknown. We further established the application of dsRNA externally targeting *agl*-2 as an RNA pesticide to slow the infection in a dose-dependent manner.

3.2 Materials and Methods

3.2.1 Fungal Culture Strains and Conditions

The wild type strain, DK3, of *S. sclerotiorum* was grown on potato dextrose agar (PDA) (Sigma) at 20-22□. The gene displaced mutants of Δ*agl*-2 and Δ*agl*-4 strains were grown on PDA amended with hygromycin B (Alfa Aesar) at 100 µg/mL as selection. Dicer mutants were produced in our previous study (Mochama et al., 2018).

3.2.2 Gene Disruption of *agl*-2 and *agl*-4

Sclerotinia sclerotiorum argonaute-like genes were predicted based on homology to those identified in *N. crassa* (Laurie et al., 2012). Published sequences of Ss1G_00334 and Ss1G_11723 in the GenBank (NCBI) are the putative argonaute genes coding for QDE-2/AGO-2 and SMS-2/AGO-4 in *N. crassa*, respectively (Figure 1). Argonaute genes were displaced by the hygromycin phosphotransferase gene (*hph*) using the split-marker homologous recombination cassettes as described before (Mochama et al., 2018). To generate the *Δagl*-2 gene displacement mutant, a 1.5 kb 5' flanking arm of *agl*-2 was PCR-amplified by primers F1-AGO2 and F2-AGO2 and a 1.5kb 3' flanking arm of *agl*-2 was PCR-amplified by primers F3-AGO2 and F4-AGO2. The *hph* gene was amplified

from pCSN43 (Fungal Genetics Stock Center) using primers PtrpC – HY and YG – TrpC to give two amplicons (1.2kb and 1.3kb) each containing part of the *hph* marker gene with an overlap (Table 1). The 5'- flank of the Δ*agl*-2 gene was then connected to the partial *hph* amplicon containing P*trp*C and the 3' flank was connected to the *hph* amplicon containing T*trp*C using the overlap extension PCR method. Eventually, an *agl*-2 gene deletion construct that included 1kb of identical sequence to the 5' flanking arm of the gene and 812bp of the 3' flanking arm sequence was derived. A similar procedure was used to generate the *Agl*-4 deletion construct with 805bp of sequence identical to the 5' flanking arm and 1.1kb of the 3' flanking arm of *agl*-4.

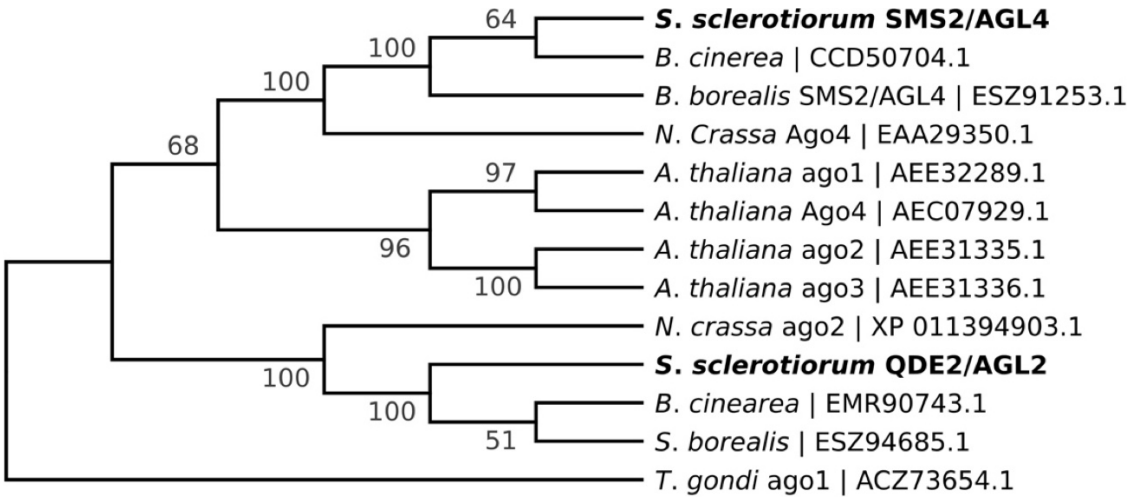

Figure 1. Phylogenetic analysis (Maximum Likelihood tree) of *agl*-2 and *agl*-4 genes depicting the relationships between the protein sequences from *S. sclerotiorum* (in bold), along with their orthologs in *B. cinerea*, *S. borealis*, *N. crassa* and *A. thaliana*. The *Toxoplasma gondii agl*-1 amino acid sequence was used as an outgroup. Bootstrap consensus was calculated based on 100 bootstrap replicates using Mega 7.0 (Kumar et al., 2016).

Table 1. Primer used in this study.

Primer Name	Sequence	Note
F1-AGO2	TGGTGAATTGTGAGTTGAATGGTG	*agl*-2 KO
F2-AGO2	ACCCAATTCGCCCTATAGTGAGTCGTGCTG CTGGATCAAAAGACAT	*agl*-2 KO
F3-AGO2	AAGCCTACAGGACACACATTCATCGTAGGT ACCTGGTCATACCTTCCGCAT	*agl*-2 KO
F4-AGO2	CAGGTCCAAGTCCTGTCCAC	*agl*-2 KO
YG-F	CGTTGCAAGACCTGCCTGAA	Both KO
PtrpC-F	ACGACTCACTATAGGGCGAATTGGGT	Both KO
TtrpC-R	TACCTACGATGAATGTGTGTCCTGTAGGCTT	Both KO
HY-R	GGATGCCTCCGCTCGAAGTA	Both KO
F1-AGO2-nested	GTTTGCAACAATCGCAGGTG	*agl*-2 KO
F4-AGO2-nested	TCTCCAACCAGCTACCGATG	*agl*-2 KO
F1-AGO4	TTTGGTCCAGGCCTTGGTTT	*agl*-4 KO
F1-AGO4-nested	TTTTCACAACGGGTTTGGGC	*agl*-4 KO
F2-AGO4	ACCCAATTCGCCCTATAGTGAGTCGTGAGC CATTAGCTTGGATATTCGCA	*agl*-4 KO

3.2.3 Fungal transformation

PEG-mediated transformation method was used to transfer the gene deletion cassettes into *S. Sclerotiorum* DK3 protoplasts as described before (Mochama et al., 2018). Fungal DNA was extracted from mycelia and PCR-amplified by the use of primers- F1 and F4, F1 and HYR, and YG2 and F4 to ascertain that argonaute genes were each displaced by the *hph* gene, confirmed by Sanger sequencing. Because *S. sclerotiorum* does not produce conidia, repeated hyphal tipping and nested PCR were necessary to derive a monokaryotic line of each targeted gene disruption to avoid mixed results from heterokaryotic mutants.

3.2.4 Complementation

To complement *agl*-2, protoplasts from the *Δagl*-2 strain was transformed with a bialaphos plasmid (pBARKS-1) cloned to express the full *agl*-2 gene flanked by 2.8 kb of 5'-upstream and 1.5 kb of 3'-downstream sequences to include the corresponding promoter and terminator. The *agl*-2 gene and flanking arms were amplified from the DNA extract of DK3 using primers F1-COMP-AGO2 and F4-COMP-AGO2 (Table 1) and inserted into the *Not*I and *BamHI* sites of pBARK-1 downstream to PTrpC and bialaphos resistance gene, *bla*1. Protoplasts and PEG-mediated transformation were the same as described earlier, except that the regeneration media was now supplemented with bialaphos at 10 μg/mL for selection. Multiple transformants were selected and hyphal-tipped several times to fresh PDA plates amended with bialaphos. PCR amplification using *agl*-2 specific primers confirmed the ectopic integration of the gene, and then four transformants were compared for the morphology on PDA between the virus-free and SsHV2-L virus-infected complemented strains.

3.2.5 Phenotypic characterization of gene deletion mutants

At least 5 replications each of DK3, *Δagl*-2, and *Δagl*-4 cultures with or without SsHV2 infections were compared for the phenotypes. Hyphal diameter was measured daily as described before (Mochama et al., 2018). A 5-mm plug was placed on the a freshly cut canola leaf. More than 3 replicates of the leaves were inoculated on moist paper towels in covered petri dishes kept on a lab bench at room temperature. Hyphal area was measured daily at 24h, 48h and 72h post inoculation.

3.2.6 In vitro dsRNA synthesis, inoculation, and confirmation of silencing by RT-qPCR

PCR amplification of the *agl*-2 target was performed using gene-specific primers with T7 promoter sequence added on both the forward primer and the reverse primer. Primers Ss-Ago2-T7p-1898F and Ss-Ago2-T7p-2065R were used (Table 1). dsRNAs were synthesized using MEGAscript T7 Transcription kit (Invitrogen) following the manufacturer's procedure. To compare the suppressing effect of dsRNA on fungal pathogenicity, a 2-day actively-growing plug in 3-mm diameter taken from the margin of a colony of *S. sclerotiorum* DK3 was placed on each canola leaf. 6 replications each of different doses of abovementioned dsRNA at 200, 400, and 800 ng was pipetted to surround an agar plug in the volume of 20 µl, taking reference from the dosage of 800 ng/20 µl published by Wang et al (Wang et al., 2016). As controls, the same volume of water, as well as dsRNA targeting *agl*-4 were pipetted to surround the agar plug on canola leaves. dsRNA targeting *agl*-4 was produced the same way as that targeting *agl*-2 but with primers Ss-Ago4-T7p-F and Ss-Ago4-T7p-R. The lesion was measured length wise and at right angle across again to obtain an average for a representative diameter two days post inoculation. The data was statistically analyzed using paired t-test; and

using one-way ANOVA (for three or more samples), and when significant effect was determined, Tukey's HSD test was performed to compare all pairs of means.

Only the lesions from 200 ng and 400 ng/20 µl were cut out to extract for total RNA using RNeasy Plant Mini Kit (Qiagen) since 800 ng/20 µl treatment does not produce lesions. RT-qPCR was performed to confirm the silencing of *agl*-2 gene in a dose-response manner using Luna Universal One-Step RT-qPCR Kit (NEB) following the manufacturer's protocol. The comparative CT method (ΔΔCT method) was used to analyze the data. The expression levels of *agl*-2 and an endogenous control (actin) were evaluated with three biological replicates and four technical replicates each. The statistical significance of observed fold-difference was analyzed by ANOVA and Tukey's test for pair-wise means separation.

3.2.7 Small RNA Libraries Preparation and Analysis of the Sequencing Results

MirVana miRNA Isolation kit (ThermoFisher Scientific) was used to extract small RNAs from 4-day-old mycelia. NEBNext small RNA Library Kit (NEB, Ipswich, MA, USA) was used to construct the libraries for sequencing. The libraries were barcoded, pooled in a single lane for 50-nt single-end reads sequencing on an HiSeq4000 at the Roy J. Carver Biotechnology Center, UIUC. Three replicates of samples from SsHV2-L virus-infected DK3 as well as four replicates (two virus-infected and two virus-free mutants) each of Δ*dcl*-1, Δ*dcl*-2, Δ*agl*-2 and Δ*agl*-4 samples were sequenced. Adaptors were trimmed by BBMap tools (Bushnell, 2014). ShortStack (Axtell, 2013) was used to identify loci producing sRNAs by clustering. The number of reads aligned to *S. sclerotiorum* and SsHV2-L genomes were computed using bowtie (Langmead et al., 2009), and further downstream analysis were performed using in-house Perl and R scripts. tRNA encoding genes were predicted by tRNAscan-SE (Lowe and Chan, 2016).

3.3 Results

3.3.1 Disruption Mutants of Argonaute-like Genes were Generated

Argonaute-like genes were disrupted directly from wild-type strain DK3 using the same approach as described before (Mochama et al., 2018). Disruption was screened by PCR amplification using F1 and F4 primers and DNA extracts from multiple transformants as the templates to rule out ectopic integration of the *hph* gene. Sanger sequencing of the PCR amplicons confirmed the integration. Once a monokaryotic mutation was obtained by hyphal-tipping and confirmed by PCR that the target genes were completely deleted, further characterizations of the mutants were carried out.

3.3.2 Effect of Argonaute-like Genes Disruption on Phenotype

The colony morphology including the growth rate and the size of the sclerotia of the argonaute mutants and the wild-type strain DK3 on PDA were compared. Single mutant *Δagl*-4 and DK3 exhibited similar growth rates, whereas the *Δagl*-2 gene displacement mutant exhibited significantly slower growth at 24 hours measured by the diameters of hyphal growth ($P<0.05$) (Figure 2A). As shown in Figure 3, at 4 days post-inoculation (dpi) (Figure 3A), no change in growth rate was observed in *Δagl*-4, whereas *Δagl*-2 mutant shows a slower growth and a reduction in the size of sclerotia produced (Figure 4). After multiple times of hyphal-tipping, four *agl*-2 complemented transformants were assayed. The complemented strains exhibited a reversal of phenotype in antiviral defense (Figure 3B).

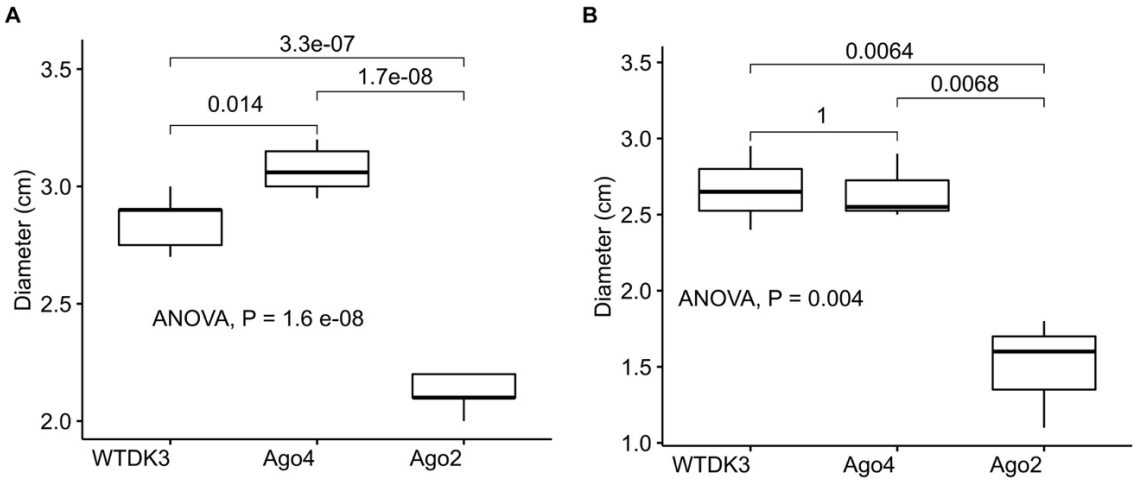

Figure 2. Average hyphal diameter of *S. sclerotioru*m wild type and argonaute gene disruption mutants (Δ*agl*-2 and Δ*agl*-4) grown (A) on PDA for 1 dpi, and (B) on detached canola leaves 2 dpi.

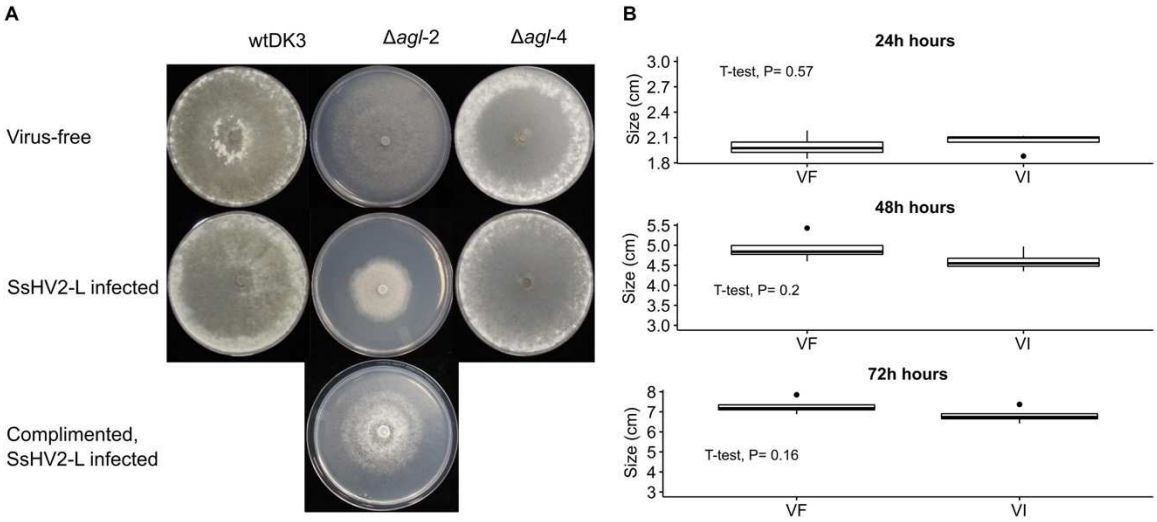

Figure 3. Colony morphology of virus-free and virus-infected gene deletion mutants. (Top row) Virus-free DK3, Δ*agl*-2 and Δ*agl*-4. (Bottom row) wild-type and mutant strains infected with hypovirus SsHV2-L. Cultures were grown for (A) 4 days on PDA. The virus-infected *agl*-2 mutant displays significantly slower growth and altered colony morphology. (B) Comparison of the complemented strains with and without virus infection (P>0.05).

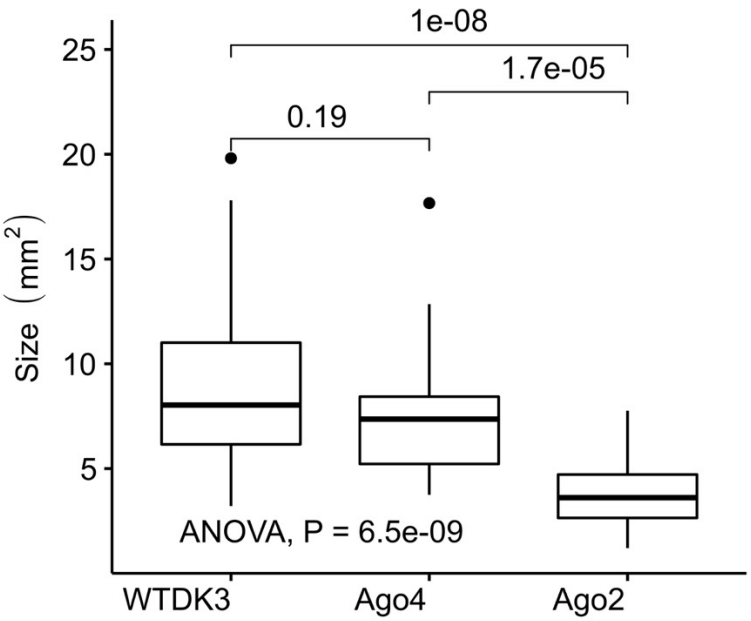

Figure 4. Comparison of sclerotial morphology in wild-type DK3 and mutant strains, Δ*agl*-2 and Δ*agl*-4. The Δ*agl*-2 mutant produces smaller sclerotia on average.

3.3.3 Effects of Argonaute-like Gene Disruptions on *S. sclerotiorum* Pathogenicity

The virulence of *S. sclerotiorum* argonaute mutants was evaluated by inoculating detached leaves with agar plugs of mycelia. Lesion size data was collected at 1, 2, and 3 dpi showed that no difference in the lesion size produced by the mutant *Δagl*-4, but a significantly smaller lesion produced by *Δagl*-2 mutant compared to those produced by DK3 (Figures 2B, 5) ($P<0.05$).

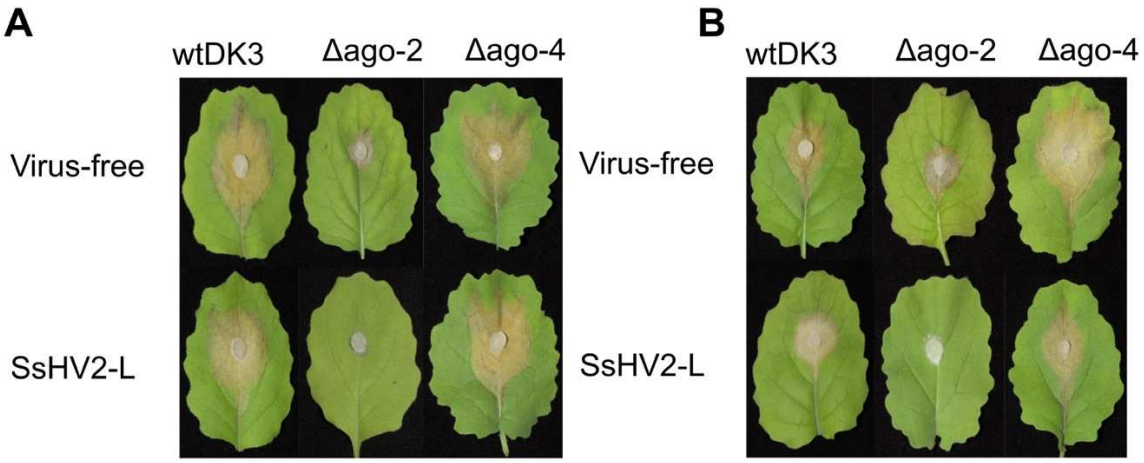

Figure 5. Virulence assays on detached canola. Plugs were taken from the edge of actively growing DK3, Δ*agl*-2 and Δ*agl*-4 cultures and inoculated onto detached leaves. Lesion size was measured (A) 2 dpi; (B) 3 dpi.

3.3.4 Effects of Argonaute Gene on antiviral defense

To examine the effect of viral infection on strains containing null-mutations of *agl*-2 and *agl*-4, mutants were transfected through hyphal fusion with SsHV2-L infected mycelia. As shown in Figure 3, no significant differences were observed in growth and morphology in the *agl*-4 mutant infected with the mycovirus compared to virus-infected DK3, whereas the *agl*-2 mutant showed a significantly debilitated growth (Figures 3, 5) ($P<0.05$).

3.3.5 In vitro synthesized dsRNA targeting *agl*-2 shows reduced virulence of *S. sclerotiorum*

Once we determined that *agl*-2 plays an important role in endogenous small RNA processing, exemplified by a debilitated growth even without virus infection, the *agl*-2 was then targeted using *in vitro* synthesized dsRNA constructs in order to disrupt the fungal small RNA processing. RT-qPCR confirmed that *agl*-2 was silenced at the level of 800 ng in 20 µl volume but not at the lower doses of 200 or 400 ng (Figure 6A). As shown in Figure 6B-D, strains in which *in vitro* 800 ng of dsRNA was applied externally

to target *agl*-2 exhibited a slower spread on canola leaves up to three days post infection compared to lower doses at 200 ng and 400 ng applied or the targeting of *agl*-4 by the corresponding dsRNA (Supplemental data).

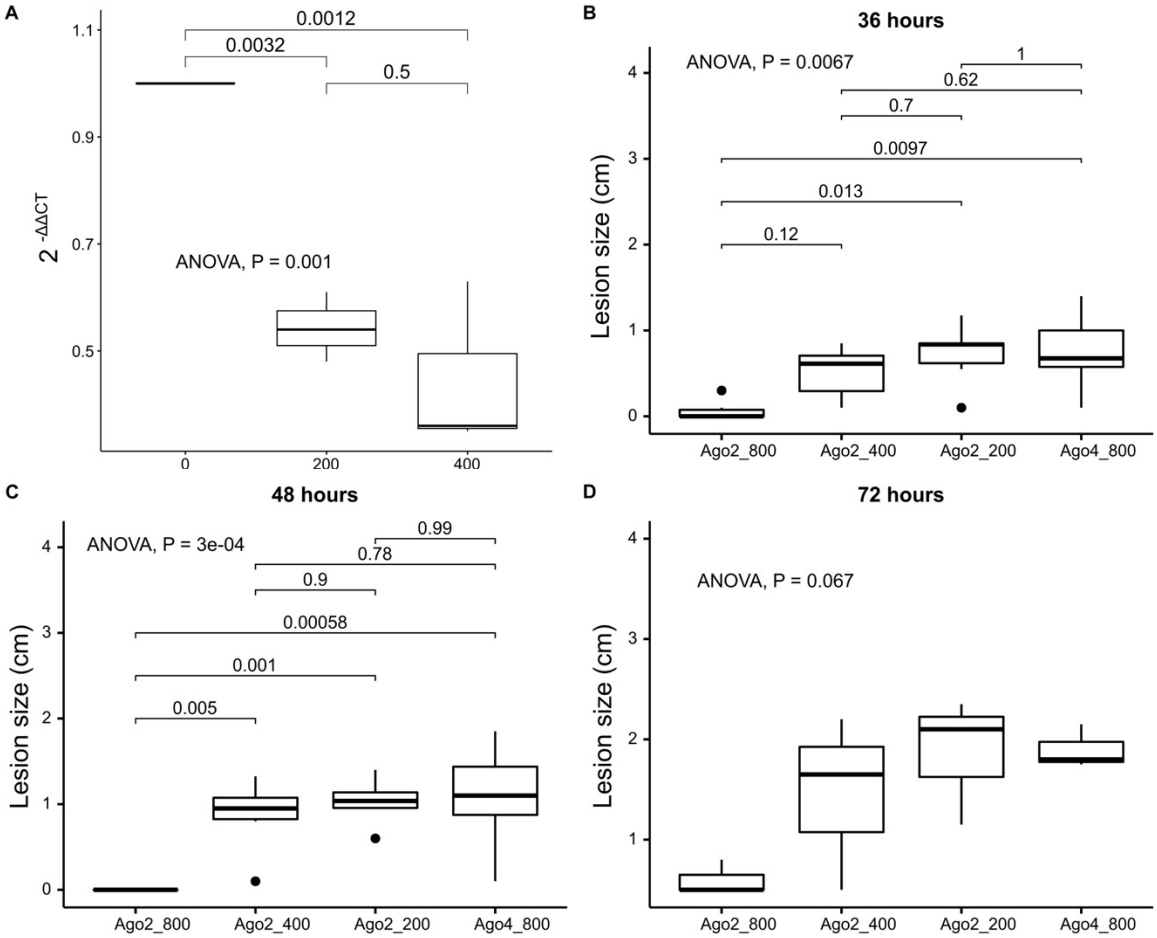

Figure 6. Effects of external RNA pesticide on inhibiting *S. sclerotiorum* from causing lesions on canola leaves comparing dsRNA targeting *agl*-2 at 800 ng/20 µl, 400 ng/20 µl, 200 ng/20 µl, dsRNA targeting *agl*-4 at 800 ng/20 µl as control (from left to right), confirmed by RT-qPCR to with reduced expression levels of *agl*-2 at 200 ng, and 400 ng, and lesion comparison at (B) 36 (C) 48, and (D) 72 hours post inoculation.

3.3.6 Profiles of sRNAs in distinct *S. sclerotiorum* strains

The raw sequence reads were uploaded to NCBI SRA database under accessions SRR8844548 (WT-1), SRR8844549 (WT-2), SRR8785208 (WT-3), SRR8785205 (Δdcl1-1), SRR8785204 (Δdcl1-2), SAMN12129781 (Δdcl1-VF1), SAMN12129782

(Δdcl1-VF2), SRR8785203 (Δdcl2-1), SRR8785202 (Δdcl2-2), SAMN12129783 (Δdcl2-VF1), SAMN12129784 (Δdcl2-VF2), SRR8785201 (Δagl2-1), SRR8785200 (Δagl2-2), SAMN12129777 (Δagl2-VF1), SAMN12129778 (Δagl2-VF2), SRR8785199 (Δagl4-1), SRR8785198 (Δagl4-2), SAMN12129779 (Δagl4-VF1) and SAMN12129780 (Δagl4-VF2). Table 2 summarized the numbers of aligned small RNA sequence reads from the mutants and the WT sample that passed the ShortStack filtering parameters to allow the clustered reads for downstream analysis.

Table 2. Numbers of aligning small RNA sequence reads from hypovirus-transfected wild type and mutants of *Sclerotinia sclerotiorum*.

	Read counts	**Percent of aligned reads**					
Samples	Filtered read	IGR (% of tRNA derived small RNA)	CDS	Retrotransposons	Mitochondria	rRNA	Other
Ago2_SsHV2L_1	6510462	46.4 (42.7%)	10.6	3.3	5.7	5.6	28.5
Ago2_SsHV2L_2	6599083	46.7 (46.73%)	9.3	2.9	5.6	5.8	29.7
Ago2_VF_1	5895665	48.4 (31.46%)	12.7	4.4	5.6	4.3	24.6
Ago2_VF_2	5646987	49.1 (32.7%)	13.5	4.8	5.2	3.9	23.5
Ago4_SsHV2L_1	15140898	58.1 (68.9%)	5.9	2.2	2.8	1.9	29.1
Ago4_SsHV2L_2	8083962	49.4 (56.8%)	8.2	3.0	4.5	8.0	26.9
Ago4_VF_1	18251848	80.1 (78.6%)	3.9	0.5	1.6	4.2	9.7
Ago4_VF_2	13039613	83.0 (80.6%)	3.5	0.5	1.8	2.8	8.4
Dcl1_SsHV2L_1	6932872	32.9 (77.6%)	2.2	0.2	1.7	24.9	38.1
Dcl1_SsHV2L_2	7040569	52.5 (62.7%)	5.3	2.3	2.6	9.2	28.1
Dcl1_VF1	9213301	50.4 (57.8%)	6.3	1.5	4.5	8.0	29.4
Dcl1_VF2	9087471	32.7 (28.6%)	5.6	0.9	4.2	19.8	36.8
Dcl2_SsHV2L_1	14427517	43.6 (62.5%)	5.6	2.3	4.6	4.9	38.9
Dcl2_SsHV2L_2	11097593	43.2 (59.2%)	6.7	3.0	4.2	5.5	37.3
Dcl2_VF1	17041328	40.6 (35.4%)	9.8	3.4	4.7	6.7	34.7
Dcl2_VF2	13619703	50.0 (59.2%)	5.6	1.8	4.7	7.2	30.8
WTDK3_SsHV2L_1	15565013	63.7 (76.0%)	5.1	1.7	3.1	3.4	23
WTDK3_SsHV2L_2	14313982	39.2 (41.4%)	9.4	4.4	2.8	1.2	43
WTDK3_SsHV2L_3	14553278	40.8 (25.4%)	11.6	4.5	8.5	2.8	31.8

A major portion of endogenous small RNAs were found to represent the same small RNAs identified from our previous study (Lee Marzano et al., 2018), predominantly tRNA halves (tRFs): tRF5-Glu(GAA), 5'-TCCGAATTAGTGTAGGGGTTAACATAACTC-3', and tRF5-Asp(GAC), 5'-TCTTTGATGGTCTAACGGTCATGATTTCC-3', derived from tRNAs delivering glutamic acid and aspartic acid at 1.1 and 1.3% of total filtered reads in average, respectively. Homologs of the abovementioned two tRFs range in size from 29-35 bases with a major peak at 33 nt as TCTTTGATGGTCTAACGGTCATGATTTCCGTCC (Figures 7A-D) (underlined are the bases when expanding the size of small RNAs up to 34 nt long). tRF5-Glu(GAA) is predicted to be produced from SS1G_14562 and SS1G_14600 on chromosomes 7 and 4, respectively, whereas tRF5-Asp(GAC) is produced from SS1G_14527 on chromosome 14. The clustering result showed that these two small RNAs were mapped solely to intergenic regions. The BLASTn search (Altschul et al., 1990) indicates their homology to specific loci on chromosomes 4, 7, 14 and 16 for tRF5-Glu(GAA), and on chromosomes 1, 5, 11, 12, and 14 for tRF5-Asp(GAC). These small RNAs and their homologs are derived from mature tRNAs and contribute to the major peak at 29 or 33 nt. Compared to the wild type (Figure 7 A), the productions of the two species were not affected by either single dicer mutations (Figures 7 B, C), nor double dicer mutations (Figure 7 D) (Mochama et al., 2018), and the stability of these small RNAs were not drastically affected by argonaute mutations (Figures 7 E, F). Therefore, the reanalyzed data of double dicer mutant (previously published in (Mochama et al., 2018)) revealed that these tRFs were not produced by either dicer.

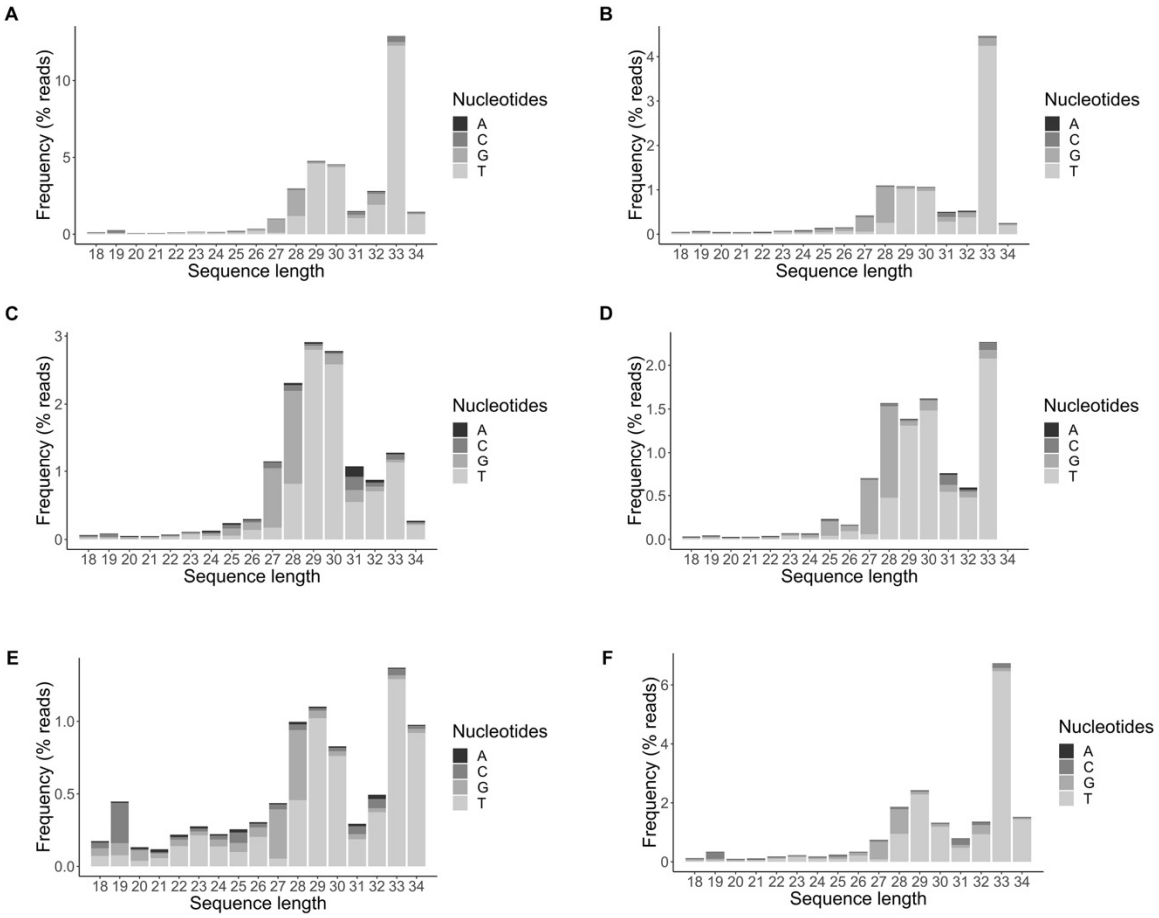

Figure 7. tRNA-derived Small RNAs profiled for their size distribution in (A) wild type strain DK3; (B) Δ*dcl*-1; (C) Δ*dcl*-2; (D) Δ*dcl*-1/*dcl*-2; (E) Δ*agl*-2; (F) Δ*agl*-4.

3.4 Discussion

Studies conducted on a number of fungal species have uncovered robust RNA silencing mechanisms with important roles in fungal antiviral defense. Similarly, this study elucidates the RNA silencing mechanisms in *S. sclerotiorum* and establishes the significant roles played by Argonaute-like genes in this devastating plant pathogenic fungus. Primarily, these findings clearly demonstrate that while the wild-type strain displayed reduced virulence following SsHV2-L virus infection (Marzano et al., 2015), RNA-silencing-deficient mutants (specifically Δ*agl*-2 mutant in this study, and previously reported Δ*dcl*-1/*dcl*-2 double mutant (Mochama et al., 2018)) displayed an even more significantly debilitated growth and reduced virulence under virus infection.

The slower growth of Δ*agl*-2 without virus infection also suggested that *agl*-2 contributes to cellular gene regulation through the prevention of RISC formation with endogenous small RNAs. Specifically, we found that the deletion of *agl*-2 gene but not *agl*-4 resulted in compromised growth and virulence prior to virus infection, suggesting the contributions made by *agl*-2 to physiological and developmental processes. The *agl*-2 mutant exhibited slower growth, smaller sclerotia, and reduced virulence. Therefore, the changes observed in the *agl*-2 mutant may be attributed to a significant reduction in small RNA loading and stabilization of endogenous small RNAs. As expected, size distribution of small RNAs is not greatly affected upon the deletions of *agl*-2 or *agl*-4 genes when the Dicers are functional.

The great debilitation observed in the Δ*agl*-2 mutant caused by virus infection was not detected in the virus-infected Δ*agl*-4. This suggests that the AGL-2 protein is solely responsible for incorporating vsiRNAs into the RISC complex as part of the viral RNA

silencing mechanism leading to the silencing of viral RNA. Argonaute proteins have been shown to associate with vsiRNAs in plants to target complementary viral mRNAs and in some cases host genes as well (Mengji et al., 2014;Carbonell and Carrington, 2015). miRNA-like molecules with possible gene regulation functions have been found to associate with fungal Argonaute proteins like the QDE-2 protein in *N. crassa* (Lee et al., 2010). Our study suggests that AGL-2 protein in *S. sclerotiorum* may also contribute to endogenous gene regulation. While AGL-4 protein's function remains unknown, it is likely to play important roles including miRNA degradation (Sheu-Gruttadauria et al., 2019). Moreover, as single argonaute mutants do not have drastic changes in small RNA stability, this suggests possible functional redundancy in the two Argonautes.

Single gene disruption mutants of *dcl*-1, *dcl*-2, *agl*-2, *agl*-4, and double dicer mutants of *dcl*-1/*dcl*-2 did not alter the accumulation of tRFs, which suggests the existence of alternative enzymes or pathways for the biogenesis of this class of small RNA in *S. sclerotiorum*. Other endonucleases exist in *S. sclerotiorum*, such as RNaseL-like endonucleases that share similarities with yeast Ire1p proteins which are said to be involved in fungal mRNA splicing (Dong et al., 2001). Another endonuclease, Rny1 in yeast, is a ribonuclease T2-like precursor, and disruption of Rny1 lead to usually large cells that are temperature-sensitive for growth in yeast (MacIntosh et al., 2001). Also, the sizes of small RNA for tRFs were much larger than the dicer-processed ~22 nt ones, supporting the speculation of different endonuclease(s) in action. Therefore, generating Rny1 and RNase L mutants to assess any disruption in the fungal growth and development and most importantly quantify the changes in the levels of tRFs will answer the pending questions brought up by this study. Moreover, the biological function of this under-characterized

class of small RNA in this major pathogen of all dicots demands further study. Questions such as whether tRFs are induced by virus infection or simply a stress response, whether they target the IGRs as Blastn results suggested, or whether tRFs can be manipulated to debilitate *S. sclerotiorum* remain to be answered in the future.

The results derived from this study pave the way for the development of new control strategies that exploit RNA silencing mechanisms. The external RNA pesticide developed suggests the occurrence of external uptake of RNA in *S. sclerotiorum*. Furthermore, host-induced gene silencing (HIGS), virus-induced gene silencing (VIGS) approaches or heterologous expression of dsRNA sprays (spray-induced gene silencing) targeting *agl*-2 in *S. sclerotiorum* are expected to be effective in reducing the virulence, adding to the tool box of disease control.

Author Contributions

AN, PM, and S-YLM conceived and designed the experiments and wrote the manuscript. PM, CF, and HS performed the experiments. AN analyzed the small RNA data.

Funding

This study was supported in part by National Sclerotinia Initiative Grant SA1800330 (to S-YLM) and SDSU startup from USDA Hatch fundSD00H606-16 project number with accession number 1009451.

Conflict of Interest Statement

The authors declare that the research was conducted in the absence of any commercial or financial relationships that could be construed as a potential conflict of interest.

Supplementary Material

The Supplementary Material for this article can be found online at: https://www.frontiersin.org/articles/10.3389/fpls.2019.00976/full#supplementary-material

References

Altschul, S.F., Gish, W., Miller, W., Myers, E.W., and Lipman, D.J. (1990). Basic local alignment search tool. *J Mol Biol* 215**,** 403-410.

Amselem, J., Cuomo, C.A., Van Kan, J.A., Viaud, M., Benito, E.P., Couloux, A., Coutinho, P.M., De Vries, R.P., Dyer, P.S., and Fillinger, S. (2011). Genomic analysis of the necrotrophic fungal pathogens Sclerotinia sclerotiorum and Botrytis cinerea. *PLoS genetics* 7**,** e1002230.

Axtell, M.J. (2013). ShortStack: comprehensive annotation and quantification of small RNA genes. *Rna*.

Baulcombe, D. (2004). RNA silencing in plants. *Nature* 431**,** 356-363.

Baulcombe, D. (2005). RNA silencing. *Trends Biochem. Sci.* 30**,** 290-293.

Bushnell, B. (2014). "BBMap: a fast, accurate, splice-aware aligner". Lawrence Berkeley National Lab.(LBNL), Berkeley, CA (United States)).

Campo, S., Gilbert, K.B., and Carrington, J.C. (2016a). Small RNA-based antiviral defense in the phytopathogenic fungus Colletotrichum higginsianum. *PLoS pathogens* 12**,** e1005640.

Campo, S., Gilbert, K.B., Carrington, J.C., and Guo, H.-S. (2016b). Small RNA-Based Antiviral Defense in the Phytopathogenic Fungus Colletotrichum higginsianum. *PLoS Pathogens* 12.

Carbonell, A., and Carrington, J.C. (2015). Antiviral roles of plant ARGONAUTES. *Current Opinion in Plant Biology* 27**,** 111-117.

Catalanotto, C., Pallotta, M., Refalo, P., Sachs, M.S., Vayssie, L., Macino, G., and Cogoni, C. (2004). Redundancy of the two dicer genes in transgene-induced posttranscriptional gene silencing in Neurospora crassa. *Molecular and cellular biology* 24**,** 2536-2545.

Dang, Y., Yang, Q., Xue, Z., and Liu, Y. (2011). RNA interference in fungi: pathways, functions, and applications. *Eukaryotic cell* 10**,** 1148-1155.

Dong, B., Niwa, M., Walter, P., and Silverman, R.H. (2001). Basis for regulated RNA cleavage by functional analysis of RNase L and Ire1p. *Rna* 7**,** 361-373.

Fulci, V., and Macino, G. (2007). Quelling: post-transcriptional gene silencing guided by small RNAs in Neurospora crassa. *Current Opinion in Microbiology* 10**,** 199-203.

Heffer Link, V., and Johnson, K. (2007). "White mold. The plant health instructor. doi: 10.1094". PHI-I-2007-0809-01).

Irvine, D.V., Zaratiegui, M., Tolia, N.H., Goto, D.B., Chitwood, D.H., Vaughn, M.W., Joshua-Tor, L., and Martienssen, R.A. (2006). Argonaute Slicing Is Required for Heterochromatic Silencing and Spreading. *Science* 313**,** 1134-1137.

Kumar, S., Stecher, G., and Tamura, K. (2016). MEGA7: Molecular Evolutionary Genetics Analysis Version 7.0 for Bigger Datasets. *Mol Biol Evol* 33**,** 1870-1874.

Langmead, B., Trapnell, C., Pop, M., and Salzberg, S.L. (2009). Ultrafast and memory-efficient alignment of short DNA sequences to the human genome. *Genome Biol* 10**,** R25.

Laurie, J.D., Ali, S., Linning, R., Mannhaupt, G., Wong, P., Güldener, U., Münsterkötter, M., Moore, R., Kahmann, R., and Bakkeren, G. (2012). Genome comparison of barley and maize smut fungi reveals targeted loss of RNA silencing components

and species-specific presence of transposable elements. *The Plant Cell* 24**,** 1733-1745.

Lee, H.-C., Li, L., Gu, W., Xue, Z., Crosthwaite, S.K., Pertsemlidis, A., Lewis, Z.A., Freitag, M., Selker, E.U., Mello, C.C., and Liu, Y. (2010). Diverse Pathways Generate MicroRNA-like RNAs and Dicer-Independent Small Interfering RNAs in Fungi. *Molecular Cell* 38**,** 803-814.

Lee Marzano, S.Y., Neupane, A., and Domier, L. (2018). Transcriptional and Small RNA Responses of the White Mold Fungus Sclerotinia sclerotiorum to Infection by a Virulence-Attenuating Hypovirus. *Viruses-Basel* 10.

Lowe, T.M., and Chan, P.P. (2016). tRNAscan-SE On-line: integrating search and context for analysis of transfer RNA genes. *Nucleic Acids Res* 44**,** W54-57.

Macintosh, G.C., Bariola, P.A., Newbigin, E., and Green, P.J. (2001). Characterization of Rny1, the Saccharomyces cerevisiae member of the T2 RNase family of RNases: Unexpected functions for ancient enzymes? *Proceedings of the National Academy of Sciences* 98**,** 1018-1023.

Marzano, S.-Y.L., Hobbs, H.A., Nelson, B.D., Hartman, G.L., Eastburn, D.M., Mccoppin, N.K., and Domier, L.L. (2015). Transfection of Sclerotinia sclerotiorum with in vitro transcripts of a naturally occurring interspecific recombinant of Sclerotinia sclerotiorum hypovirus 2 significantly reduces virulence of the fungus. *Journal of virology***,** JVI. 03199-03114.

Mengji, C., Peng, D., Xianbing, W., Yun-Qi, Y., Yan-Hong, Q., Wanxiang, L., Amit, G.-O., Changyong, Z., Yi, L., and Shou-Wei, D. (2014). Virus infection triggers widespread silencing of host genes by a distinct class of endogenous siRNAs in Arabidopsis. *Proceedings of the National Academy of Sciences* 111**,** 14613.

Mochama, P., Jadhav, P., Neupane, A., and Marzano, S.-Y.L. (2018). Mycoviruses as Triggers and Targets of RNA Silencing in White Mold Fungus Sclerotinia sclerotiorum. *Viruses* 10.

Poulsen, C., Vaucheret, H., and Brodersen, P. (2013). Lessons on RNA silencing mechanisms in plants from eukaryotic argonaute structures. *The plant cell* 25**,** 22-37.

Qihong, S., Gil, H.C., and Donald, L.N. (2009). A single Argonaute gene is required for induction of RNA silencing antiviral defense and promotes viral RNA recombination. *Proceedings of the National Academy of Sciences* 106**,** 17927.

Segers, G.C., Zhang, X., Deng, F., Sun, Q., and Nuss, D.L. (2007). Evidence that RNA silencing functions as an antiviral defense mechanism in fungi. *Proceedings of the National Academy of Sciences* 104**,** 12902-12906.

Sheu-Gruttadauria, J., Pawlica, P., Klum, S.M., Wang, S., Yario, T.A., Oakdale, N.T.S., Steitz, J.A., and Macrae, I.J. (2019). Structural Basis for Target-Directed MicroRNA Degradation. *Available at SSRN 3318944*.

Trieu, T.A., Calo, S., Nicolás, F.E., Vila, A., Moxon, S., Dalmay, T., Torres-Martínez, S., Garre, V., and Ruiz-Vázquez, R.M. (2015). A Non-canonical RNA Silencing Pathway Promotes mRNA Degradation in Basal Fungi (An RdRP-Dependent Degradation Mechanism of mRNA). 11**,** e1005168.

Wang, M., Weiberg, A., Lin, F.-M., Thomma, B.P., Huang, H.-D., and Jin, H. (2016). Bidirectional cross-kingdom RNAi and fungal uptake of external RNAs confer plant protection. *Nature plants* 2**,** 16151.

Waterhouse, P.M., Wang, M.B., and Lough, T. (2001). Gene silencing as an adaptive defence against viruses. *Nature* 411**,** 834-842.

Yu, J., Lee, K.-M., Cho, W.K., Park, J.Y., and Kim, K.-H. (2018). Differential Contribution of RNA Interference Components in Response to Distinct Fusarium graminearum Virus Infections. *Journal of Virology* 92.

Zhang, D.-X., Spiering, M.J., and Nuss, D.L. (2014). Characterizing the roles of Cryphonectria parasitica RNA-dependent RNA polymerase-like genes in antiviral defense, viral recombination and transposon transcript accumulation. *PloS one* 9**,** e108653.